INTEGRINS ACT WITH ROBO TO ESTABLISH HEART CELL POLARITY

DROSOPHILA INTEGRINS ACT IN CONJUNCTION WITH ROBO TO ESTABLISH HEART CELL POLARITY

By

LUZ DE LOURDES VAZQUEZ PAZ, B.Sc. (Hons.)

A Thesis
Submitted to the School of Graduate Studies
in Partial Fulfilment of the Requirements
for the Degree
Master of Science

McMaster University

MASTER OF SCIENCE (2010)
(Biology)

McMaster University
Hamilton, Ontario

TITLE: Drosophila Integrins Act in Conjunction with Robo to Establish Heart Cell Polarity

AUTHOR: Luz de Lourdes Vazquez Paz, B.Sc. (Hons.) (McMaster University)

SUPERVISOR: J. Roger Jacobs, Ph.D., Professor , McMaster University

NUMBER OF PAGES: viii, 114

ABSTRACT

The *Drosophila* heart arises from the migration and subsequent fusion of bilateral rows of cardioblasts into a single dorsal vessel at the midline. Previous studies have demonstrated that the coordinated migration, and formation of a lumen in the Drosophila heart requires signalling by Slit, which is secreted by the cardioblasts and binds to Robo receptors on the same cells. Cardioblasts also express a single Integrin dimer, αPS3/βPS1, and as key factors in cell migration and cell-matrix adhesion, are required for assembly of the heart. Embryos heterozygous for a null allele of *slit* or *scab* have normal heart development however when gene dosage in the Slit and Integrin pathways are altered simultaneously more than additive effects such as delayed migration of cardial cells, cell clumping and midline crossing, suggest that the two pathways intersect upon a common function. This thesis demonstrates that reduced Integrin function delays the acquisition of cell polarity by heart cells and prevents lumen formation. Furthermore, localization of Robo to the heart lumen requires Integrin function, and reciprocally, Robo function is required for proper Integrin distribution. These findings support a role for Integrins working in conjunction with Robo in the establishment of heart cell polarity and revealed the complexity of this interaction.

ACKNOWLEDGEMENTS

First I would like to thank my supervisor, Dr. Roger Jacobs, for taking a chance on me and giving me the opportunity to complete a Master's degree in his lab even before I got funded. Roger, I thank you for all the great talks, the guidance, encouragement and enthusiasm you brought to my project. In times of doubt you reassured me and in times of discouragement you motivated me. You believed in me and pushed me to be a better more critical thinker. In your lab I developed not only scientific skills, but skills that are invaluable for life and for that I will be forever grateful.

To Dr. Ana Campos, thank you for your guidance and supervision. I appreciate the time you set aside to supervise my project. You always had useful and helpful input that helped me be more critical of my data. You taught me that ignorance is an opportunity to learn more and I will always remember that lesson.

My graduate experience would not have been what it was without all the love and support from those who have been a part of my life during these three years. To my lab colleagues past and present I thank you for all the laughs and knowledge we shared, my lab experience was certainly enriched because of all of you. To Dr. Mihaela Georgescu, thank you for your guidance and advice, you were always there to teach me something new. To the members of the Campos lab, thanks for all the great times spent looking through a microscope; you helped make the time "fly" by and to Xiao Li for looking after me and your delicious food.

To my friends, grad school was well worth it since it meant I got to meet you all. All the coffees, the laughs, the lunches, the stories and lest-not-forget our Phoenix escapades, I have thoroughly enjoyed getting to know each of you and each one has filled my life with memories that will remain with me forever. Thank you for your friendship.

To Sarah O'Sullivan, you were my support outside of my life in the lab. I could not have accomplished this without you. Your friendship has been invaluable to me and it has made my life in Canada feel as if I weren't so far away from home. Thank you for always being there.

Finally, I would like to thank my family. Your never-ending encouragement and support has provided me with the confidence to seek new challenges and move forward knowing that I always have you to lean on. To my parents, I thank you for always believing in me, for teaching me to work hard and always encouraging me to follow my dreams even if that has led me to places far away from you. To my sister and nieces, your love and kindness have always been there at a moment's notice to brighten up my days. To my grandparents, you were always so loving and proud of me, I miss you. To Taylor, having you by my side has meant more than words can say, you have been there for support, encouragement and inspiration. I look forward to the adventures that await us in the future.

TABLE OF CONTENTS

TITLE PAGE I
DESCRIPTIVE NOTE II
ABSTRACT III
ACKNOWLEDGEMENTS IV
TABLE OF CONTENTS VI
LIST OF ILLUSTRATIONS VII

CHAPTER ONE: INTRODUCTION 1
1.1 Overview of the *Drosophila* heart morphogenesis 2
1.2 Cardioblast migration and dorsal closure 4
1.3 Cell Polarity 5
1.4 Lumen Formation 8
1.5 Cell signalling 12
1.51 Slit and Robo 12
1.52 Syndecans 15
1.6 Integrins 16
1.61 Integrins in the heart 20

CHAPTER TWO: METHODS 23
2.1 Fly Stocks 23
2.2 Embryo collection and fixation 25
2.3 Immunohistochemistry 26
2.31 Immunolabelling 26
2.32 Antibodies 27
2.4 Mounting and Imaging 27
2.5 Rabbit Polyclonal anti-αPS3 Antibody Generation 30
2.51 Preparation of His tagged αPS3 construct 30
2.52 αPS3 His Tagged Protein Induction and Purification 30
2.53 Immunization 32
2.6 Preparation of Crude Protein Lysate from *Drosophila* Tissue 33
2.61 Protein Lysate Extraction from *Drosophila* Embryos 33
2.62 Protein Lysate Extraction from *Drosophila* Heads 34
2.7 Heat Shock 34
2.8 Western Blot Analysis 35
2.9 RNAi Lethality 36
2.10 *UAS-scb* Rescue of *scb*^{2} Null Embryos 36
2.11 Scoring of Heart Mutant Phenotypes 37

CHAPTER THREE: RESULTS 38
3.1 Generation of a polyclonal antibody to visualize Integrin localization in the *Drosophila* heart 38
3.2 Altered Integrin expression results in heart assembly defects 40
3.21 Embryos expressing a cytoplasmically truncated αPS3 Integrin have severe perturbations in heart development 42
3.3 αPS3 is required for the formation of the heart lumen 45
3.4 Integrins are required for Slit and Robo apicalization 45
3.5 Overall cell polarity of cardioblasts is not disrupted in the absence of αPS3 51
3.6 Over-expression of αPS3 partially restores Robo and Slit localization to the apical membrane of *scab* cardioblasts 55
3.7 Requirement for Robo in Integrin localization 55
3.8 RNA interference mediated knockdown of αPS3 and βPS1 56

CHAPTER FOUR: DISCUSSION 66
4.2 Integrins are required for heart and lumen formation 68
4.21 Effects of Dorsal Closure in heart analyses 69
4.3 Integrins may have a role in cardioblast cell migration 71
4.4 Integrins may have an adhesive function in the heart 72
4.5 Integrins may be required for Slit and Robo localization and/or stabilization to the apical membrane of cardioblasts and are downstream of polarizing signals 73
4.6 Integrins may be downstream of Robo's polarizing signal 76
4.7 Cell autonomy 77
4.8 Concluding Remarks and Future Directions 78

BIBLIOGRAPHY 80
APPENDIX 1 88
APPENDIX 2 101

LIST OF ILLUSTRATIONS

CHAPTER 1

Figure 1.1 Formation and structure of the dorsal vessel in *Drosophila* 7
Figure 1.2 Models of lumen formation 11

CHAPTER 2

Table 2.1 Mutations and transgenic lines 24
Table 2.2 Primary antibodies 28
Table 2.3 Secondary Antibodies 29

CHAPTER 3

Figure 3.1 Altered αPS3 expression phenotypes in the *Drosophila* heart 44
Figure 3.2 αPS3 is required for lumen formation 48
Figure 3.3 αPS3 is required for Slit and Robo concentration in the lumen 50
Figure 3.4 Cell polarity markers in wild type and *scab* mutant embryos 54
Figure 3.5 Expression of αPS3 partially restores Slit and Robo localization 60
Figure 3.6 Integrins are mislocalized in the absence of Robo 62
Figure 3.7 Apicalization of Slit and Robo requires Integrins cell autonomously 64
Table 3.1 Frequency of heart assembly defects in αPS3 mutants 65
Table 3.2 Frequency of heart assembly defects in RNA interference experiments 65

APPENDIX 1

Figure A1.1 The αPS3 integrin *scab* interacts genetically with *slit* in a dosage dependent manner 90
Figure A1.2 *slit* interacts in a dosage dependent manner with genes required for adhesion 92
Figure A1.3 *slit* interacts genetically with downstream effectors of integrin function 94
Figure A1.4 Integrins function to coordinate cardial cell morphogenesis in an adhesive nature 96
Figure A1.5 The αPS3 integrin *scab* interacts genetically with genes required for Robo signalling 98
Figure A1.6 The *sli/scb* dorsal vessel phenotype is not due to a defect in dorsal closure 100

APPENDIX 2

Figure A2.1 Slit and Robo localization in wild type and scb01288 103
Figure A2.2 Characterization of the αPS3 polyclonal antibody 105
Figure A2.3 RNAi mediated knockdown of αPS3 and βPS1 107
Figure A2.4 Localization of the cell junctional marker Par6 109
Figure A2.5 Sequence Alignment of pUAST-*scab* and CDS 111
Table A2.1 Adult viability analysis of transgene over-expression 112
Table A2.2 Adult viability analysis of transgene over-expression in a *scb2* background 113
Table A2.3 Adult viability analysis of RNAi over-expression at 29°C 114
Table A2.4 RNAi embryonic lethality 114

Chapter One: INTRODUCTION

Some years ago I learned of a man named Vivien Thomas and his contribution to treat the blue baby syndrome (Tetralogy of Fallot). It occurred to me that even though we may be able to treat many congenital heart defects the developmental and molecular processes leading to these still remain unknown. Therefore, understanding the mechanisms that give rise to the heart should be of fundamental importance in developmental biology.

The vertebrate and the *Drosophila* hearts look and function quite differently; nevertheless there are remarkable developmental similarities during embryogenesis (Chen & Fishman, 2000). For example, they both share a mesodermal origin and initially assemble into a linear tube (Bodmer & Venkatesh, 1998). Many of the basic transcriptional programs for cardiac specification and differentiation are conserved (Cripps & Olson, 2002). While the vertebrate heart is decidedly more complex than that of the fruit fly, it is thanks to the conservation of many of the embryological events involved in heart formation that we have been able to advance the understanding of the underlying molecular events of heart formation (Cripps & Olson, 2002; Medioni et al., 2009; Tao & Schulz, 2007).

1.1 Overview of the *Drosophila* heart morphogenesis

The simple and structured morphology of the *Drosophila* dorsal vessel allows for detection of morphological alterations due to changes in regulatory pathways or genes of interest. It is comprised of a small, known number of cardial cells which can be easily and individually identified and analyzed at high resolution. In addition, the *Drosophila* embryo is able to develop without a functional heart, thus facilitating the detailed analysis of mutant phenotypes on the mature organ (Cripps & Olson, 2002; Medioni et al., 2009)

Cardiac cell progenitors are derived from lateral mesoderm, which, during gastrulation, invaginate and spread laterally to form a monolayer in close contact with the overlying ectoderm (embryonic stage 9). This cell spreading is needed for the mesoderm to receive instructions from the dorsal ectoderm. Fibroblast growth factor (FGF) signals Pyramus and Thisbe from the ectoderm through the Heartless receptor on the mesoderm, induce a subset of dorsal mesodermal cells in each hemisegment to acquire a cardial fate (Kadam, McMahon, Tzou, & Stathopoulos, 2009; Klingseisen, Clark, Gryzik, & Muller, 2009). From embryonic stages 12-17, fated cells from each side of the embryo migrate to the dorsal midline (Fig. 1.1A) (Cripps & Olson, 2002). During this dorsal migration, activation of specific gene networks results in the specification of different cell types that give rise to the mature dorsal vessel by embryonic stage 17, which is comprised of two central rows of cardial cells that form the contractile tube surrounded by

non-muscle pericardial cells (Fig. 1.1B) (Cripps & Olson, 2002). The mature heart pumps blood anteriorly toward the brain; the blood then drains posteriorly until it re-enters the heart through inflow tracts termed ostia. The heart tube is affixed to the dorsal wall by seven pairs of segmentally repeated alary muscles (Cripps & Olson, 2002; Tao & Schulz, 2007).

Among the cardioblasts, there are genetically distinct cells that are segmentally patterned along the anterior-posterior axis of the embryo. Each segment consists of six pairs of cardioblast cells, four in each segment express the gene *tinman* and the remaining two express the gene *seven-up*, both encoding transcription factors that establish cell fate (Gajewski, Choi, Kim, & Schulz, 2000). Upon the dorsal vessel as a whole there is an additional anterior-posterior axis. The posterior two segments form the heart proper, and this is structurally and functionally distinct from the anterior region, termed the aorta (Cripps & Olson, 2002; Tao & Schulz, 2007). The heart and aorta are separated by a pair of cells that form a cardiovascular valve. In addition, the ostia through which hemolymph enters the circulation are located exclusively in the heart during embryonic and larval stages (Fig. 1.1B) (Cripps & Olson, 2002).

Proper heart morphogenesis is dependent upon intracellular signalling and regulated gene expression. Multiple signalling pathways are essential to heart formation such as Fibroblast growth factor (FGF) necessary for mesodermal spreading and specification, Decapentaplegic (Dpp) also involved in fate specification by regulating *tinman* expression, Wingless (Wg) and Notch are

required for cardiogenic specification from the dorsal mesoderm, Hedgehog (Hh) for the process of cell differentiation, the details of these pathways are, however, among beyond the scope of this thesis project.

1.2 Cardioblast migration and dorsal closure

Dorsal vessel morphogenesis requires the concerted regulation of cardioblast alignment, migration and polarization to generate a functional organ (Tao & Schulz, 2007). At stage 12, specified cardioblasts align as continuous rows of cells on both sides of the embryo. Misalignment of these cells often leads to heart structural defects. Once the cells are properly aligned, the two rows migrate dorsally towards the midline. This migration coincides with the process of dorsal closure where the ectoderm migrates to enclose the dorsal part of the embryo. The cells of the epidermis form a leading edge and lead the migration of the lateral epidermis towards the midline. Eventually, around stage 15 the two leading edges meet and fuse, enclosing the gut and the transient tissue known as the amnioserosa (Rugendorff, Younossi-Hartenstein, & Hartenstein, 1994). The migration of the cardial and pericardial cells occurs in close proximity to the dorsal ectoderm. Thus processes involved in dorsal closure may also affect cardioblast migration. It has been hypothesized that cell-cell and cell-ECM interactions act in the concerted migration of the overlying ectoderm and the heart precursors (Chartier, Zaffran, Astier, Semeriva, & Gratecos, 2002). The cardioblasts and the pericardial cells are close enough to the overlying ectoderm

(Rugendorff et al., 1994) to engage in these interactions via the ECM that surrounds the heart (Zaffran et al., 2006).

1.3 Cell Polarity

Prior to reaching the midline, the cardioblast precursor cells undergo mesenchymal-to-epithelial transition (MET) and thus become polarized {{92 Rugendorff, A. 1994; 102 Santiago-Martinez, Edgardo 2008}}. Subsets of membrane and cytoskeletal proteins localize to distinct regions of the cell surface to create the apical and basal-lateral membrane domains (Drubin & Nelson, 1996) that grant to the cells their epithelial polarity. Cell polarization is an important prerequisite for migration and alignment of heart cells since mutations in genes required for cardial cell polarization such as *pericardin*, *slit*, *robo* to mention a few, lead to heart assembly defects (Chartier et al., 2002; MacMullin & Jacobs, 2006; Qian, Liu, & Bodmer, 2005)

Heart cells have been assumed to possess an apical-basal polarity typical of epithelial cells (Frémion et al., 1999). Recently, however, there is evidence that polarity of cardial cells might be more complex. It has been suggested that in heart cells the luminal surface which typically expresses apical markers has a polarity resembling that of a basal domain because of the expression of basal components such as Slit, integrins and extracellular matrix proteins Laminin A and Trol (Medioni, Astier, Zmojdzian, Jagla, & Semeriva, 2008).

Figure 1.1: Formation and structure of the dorsal vessel in *Drosophila*.

The *Drosophila* heart arises from the dorsal migration and subsequent fusion of bilateral rows of cardioblasts into a single tube at the midline. [A] At the beginning of embryogenesis mesoderm is specified on the ventral side of the embryo (purple). By stage 8, the mesoderm cells have invaginated and spread dorsally along the inside of the ectoderm. At stage 9 the *tinman* expressing dorsal mesoderm becomes restricted (shown in purple, the rest of the mesoderm is shown in green). At stage 11, the visceral mesoderm precursors (green) move to the interior of the embryo, leaving just the Tinman-expressing heart precursors close to the epidermis (purple). By stage 12 distinct heart precursors form a continuous row of cardioblasts on each side of the embryo which will migrate dorsally in close contact with the overlying ectoderm. At stage 17, the cardioblasts come together forming the dorsal vessel at the midline. Anterior is to the left. [B] The dorsal vessel consists of two inner rows of cardioblast cells which express either *tin* (green) or *svp* (red). The posterior end of the dorsal vessel (the heart proper) has a larger lumen than the aorta. The cardial cells are surrounded by pericardial cells shown in yellow and the whole structure is held in place by the alary muscles (blue). Frontal view with anterior to the top. Adapted from (Cripps & Olson, 2002). Reprinted with permission from Elsevier.

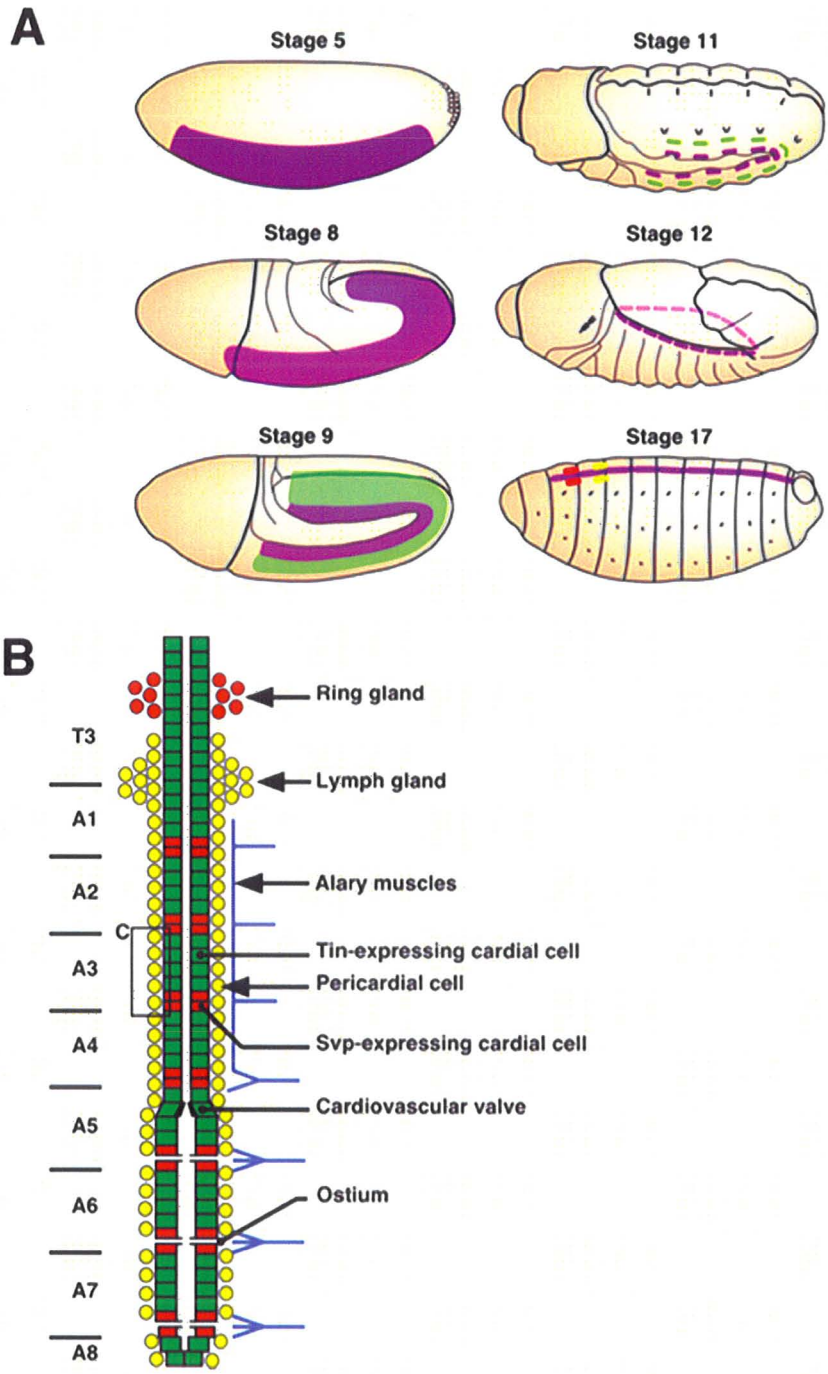
A
Stage 5
Stage 11
Stage 8
Stage 12
Stage 9
Stage 17
B
Ring gland
T3
Lymph gland
A1
A2
Alary muscles
C
Tin-expressing cardial cell
A3
Pericardial cell
A4
Svp-expressing cardial cell
A5
Cardiovascular valve
A6
Ostium
A7
A8

1.4 Lumen Formation

In the last stages of *Drosophila* heart development a lumen forms between the apical surfaces of contralateral cardioblast cells. Lumen formation is an essential process during vascularisation. Figure 1.2 depicts some of the models proposed for lumen formation in the trachea, malpighian tubules and the heart (Andrew & Ewald, 2010). The vascular lumen formation involves the formation of apical vesicles within individual cells or between subsets of cells at sites of adhesion. These vesicles will fuse together with the plasma membrane to produce a lumen between cells (Fig. 1.2A) (Andrew & Ewald, 2010; B. Lubarsky & Krasnow, 2003a) however the cellular and molecular mechanisms that drive this process are poorly understood. Changes in cell adhesion and cell-cell contact, such as E-cadherin mediated adhesion, must also be regulated during this process (Dejana, Bazzoni, & Lampugnani, 1999). The fruit fly embryonic heart is a polarized epithelial tube resembling a capillary however little is known about the process of lumen formation in this organ.

Several genes have been shown to be involved in the process of heart lumen formation. DE-cadherin (*shg*) is expressed in the membrane of cardioblasts (Haag, Haag, Lekven, & Hartenstein, 1999). When DE-cadherin is absent cardioblast still align properly but do not attach to each other and fail to form a lumen. Recent research has shown that Slit and its receptor Roundabout (Robo) are required for heart lumen formation (MacMullin & Jacobs, 2006; Medioni et al., 2008; E. Santiago-Martinez, Soplop, & Kramer, 2006). Slit is an

extracellular matrix (ECM) protein that binds and activates the Roundabout (Robo) family of transmembrane receptors (Kidd, Bland, & Goodman, 1999; J. M. Rothberg, Jacobs, Goodman, & Artavanis-Tsakonas, 1990). In the *Drosophila* central nervous system, expression of *slit* by the midline glial cells creates a repulsive cue for *robo*-expressing central nervous system axons (Battye, Stevens, & Jacobs, 1999; Kidd et al., 1999). Recently there has been genetic evidence for a repulsive role for Slit in the heart (Medioni et al., 2008; E. Santiago-Martinez, Soplop, Patel, & Kramer, 2008). Data suggest that Slit/Robo signalling is required at the apical membrane of cardioblasts for inhibition of DE-cadherin mediated adhesion and to promote the cell shape changes required for lumen formation (Medioni et al., 2008; E. Santiago-Martinez et al., 2008).

Figure 1.2: Models of lumen formation

Tubes are formed by polarized epithelial cells with their apical membrane surface facing the lumen space, and their basal surface exposed to the extracellular matrix. Several models of epithelial tube formation have been described however there is little known about *Drosophila* heart lumen formation. Shown in this diagram are some of the current models for lumen formation.

[A] In cord hollowing, the cells become polarized and small cytoplasmic vesicles form at the apical membrane at the sites of cell contact. Vesicles then fuse with each other and create a single common lumen. [B] In cell hollowing, large vesicles composed of apical membrane are created within individual cells. These vesicles fuse with each other intracellularly and eventually with the plasma membrane to form common apical lumen. During the expansion of the *Drosophila* tracheal branches, vesicles carrying apical markers are thought to fuse together at the apical membrane, driving lumen expansion (B. Lubarsky & Krasnow, 2003b). [C] Lumen formation in the fruit fly heart has specific sites of adhesion between contralateral cardial cells. It has been proposed that Slit/Robo signalling is required to restrict DE-cadherin accumulation to the dorsal and ventral attachment points of the cardial cells allowing for the formation of a lumen. Adapted from (Andrew & Ewald, 2010) and (E. Santiago-Martinez et al., 2008; E. Santiago-Martinez et al., 2006). Reprinted with permission pending.

A) Cord Hollowing

B) Cell hollowing

C) *Drosophila* heart lumen

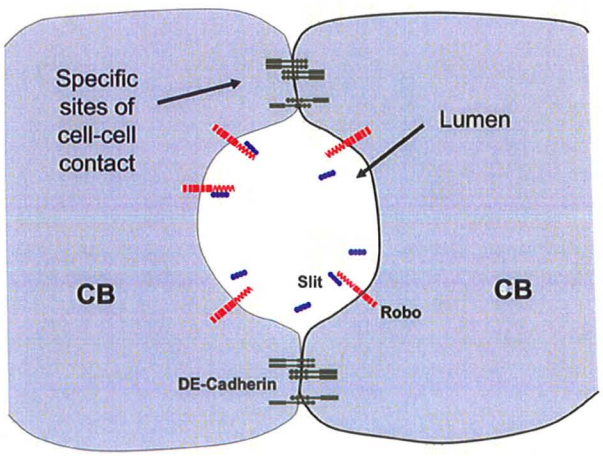

1.5 Cell signalling

1.51 Slit and Robo

Slit is a secreted glycoprotein that exhibits extracellular matrix protein motifs such as leucine-rich repeats (LRR) and epidermal growth factor (EGF)-like repeats (J. M. Rothberg et al., 1990). Each of these motifs has been implicated in protein-protein interactions as part of an extracellular domain in a variety of other proteins. The highly conserved Slit protein acts as both an attractive and repulsive guidance signal for migrating cells in a variety of different tissues(Kramer, Kidd, Simpson, & Goodman, 2001; E. Santiago-Martinez et al., 2006; Wong, Park, Wu, & Rao, 2002). Slit processes are mediated by its receptor Roundabout (Robo), in target cells (Kidd et al., 1998). In vertebrates, there are four known Robo receptors for Slit: Robo, Robo2, Robo3 and Robo 4 (Huminiecki, Gorn, Suchting, Poulsom, & Bicknell, 2002; Kidd et al., 1998; Yuan, Cox, Dasika, & Lee, 1999) while three *robo* genes have been identified in *Drosophila*, *robo*, *robo2* and *robo3* (Kidd et al., 1999; Rajagopalan, Vivancos, Nicolas, & Dickson, 2000; Simpson, Bland, Fetter, & Goodman, 2000).

The role of Slit/Robo signalling in the nervous system has been well established. Binding of Slit to Robo triggers cytoskeletal rearrangements within the axon growth cone resulting in axon repulsion (Dickson & Gilestro, 2006). In the nervous system there is a strong genetic interaction between *slit* and *robo* and between *slit* and genes required for Robo signalling (Stevens & Jacobs, 2002). Genetic studies in diverse model organisms suggest that vasculogenesis

and axon guidance share common pathways (Autiero, De Smet, Claes, & Carmeliet, 2005). This is supported by the expression of axonal guidance cues like Slit in the *Drosophila* heart (J. M. Rothberg, Hartley, Walther, & Artavanis-Tsakonas, 1988). The developing heart is the only known tissue where Slit and Robo are expressed in the same cell (MacMullin & Jacobs, 2006; Qian et al., 2005) which provides a new model for attractive and repulsive signalling. A previous student in the Jacobs lab, Allison MacMullin, did not observe genetic interactions between *slit* and *robo* in the heart. However a strong genetic interaction between *slit* and integrins, particularly αPS3, and between *slit* and genes required for adhesion and integrin signalling was reported (MacMullin & Jacobs, 2006) (Appendix 1, Fig.A1.1 and A1.2). This suggests that the functional relationship between Slit and Robo in the heart involves other signals, such as adhesion signals (MacMullin & Jacobs, 2006).

In the heart, before dorsal closure, Slit is present throughout the cytoplasm of the cardioblast cells (Qian et al., 2005). At stage 16, Slit begins to accumulate at the dorsal midline between the contacting cardioblasts (Qian et al., 2005). Like Slit, Robo is present in the cytoplasm of cardioblasts before dorsal closure and begins to accumulate apically by stage 16 (Qian et al., 2005). The innermost cardioblast cells express only Robo, whereas the flanking pericardial cells express both Robo and Robo2. Robo2 however, is only localized to the pericardial cells and remains that way before and after dorsal closure (Qian et al., 2005).

Mutations in *slit* result in heart defects, where the two rows of cardioblasts fail to align properly at the dorsal midline. There are visible defects in cell migration such as delays, midline crossings and twists and/or failure to contact their contralateral partners (blisters). In addition, interruptions of the continuous rows of cells can be observed often leading to breaks, cell clumps and irregular alignment of cells (MacMullin & Jacobs, 2006). These data suggest a role for Slit in cardial cell migration. Interestingly, previous research by Allison MacMullin showed that heart morphology was partially restored in *slit* mutants that express a *slit* transgene unable to bind Robo suggesting that direct Slit/Robo interaction may not be essential to *slit*'s function in the heart.

On the other hand, embryos mutant for *slit* also fail to form a heart lumen (MacMullin & Jacobs, 2006; Medioni et al., 2008; E. Santiago-Martinez et al., 2008). Mislocalization of Slit outside the cell's apical domain causes ectopic lumen formation. This effect is suppressed in *robo* mutants, which indicates *robo*'s requirement for this process (E. Santiago-Martinez et al., 2008). It is possible that there are different requirements for Slit signalling in heart formation, an early role mediated by adhesion signals which controls cell migration to the midline and a later role mediated by Robo to form a heart lumen.

In addition Slit and Robo play a role in heart cell polarity acquisition and maintenance. In wild type embryos Discs-Large (Dlg) and α-Spectrin have a basal-lateral polarity during cardioblast migration and an apical-lateral polarity once the cardioblasts make contact with their contralateral partners. In *slit* and

robo mutants Dlg and α-Spectrin localization is disrupted, however the polarity phenotype is observed only upon heart assembly, suggesting that Slit and Robo are not required for initiating polarity but rather for correctly switching the polarity from basal-lateral to apical-lateral (Qian et al., 2005).

1.52 Syndecans

To date, two types of cellular receptors for Slits have been identified: Robos and Syndecan. (Johnson et al., 2004; P. Steigemann, Molitor, Fellert, Jäckle, & Vorbrüggen, 2004). Syndecans are transmembrane heparan sulphate proteoglycans (HSPGs) that frequently act as co-receptors for extracellular matrix molecules and growth factors to initiate cytoplasmic signals in response to a range of extracellular cues (Bass, Morgan, & Humphries, 2009; Xian, Gopal, & Couchman, 2010).

The *Drosophila* homolog of Syndecan (*sdc*) is required for proper Slit signalling in the nervous system (P. Steigemann, Molitor, Fellert, Jackle, & Vorbruggen, 2004). It has been proposed that Syndecan works to amplify the Slit signal through Robo by concentrating Slit in the target cells (Chanana, Steigemann, Jackle, & Vorbruggen, 2009). In addition, it has also been shown that Syndecan localization to developing axons overlaps heavily with Robo receptor expression and that Slit distribution is abnormal in Syndecan mutants (Johnson et al., 2004). Biochemical data suggest that Slit, Robo and Syndecan interact with each other through the formation of a ternary complex (Chanana et al., 2009).

In the case of ECM molecules, the syndecans can be co-receptors with integrins affecting cell adhesion, migration, and matrix assembly (Xian et al., 2010). Currently the Jacobs lab is exploring the contribution of Syndecan to the development of the *Drosophila* heart and found that Syndecan may be necessary for proper specification of the heart precursors perhaps through the FGF receptor Heartless. A later function involves Syndecan in heart lumen formation as *sdc* mutants fail to develop a lumen and fail to apicalize Slit and Robo, suggesting a role for Syndecan in stabilizing and polarizing the complex (unpublished). As with Slit, *sdc* was also shown to have strong genetic interactions with the αPS3 integrin and with integrin ligands causing severe defects in heart morphology (unpublished). Since Slit/Robo signalling as well as integrins are required during heart assembly for cardiac cell alignment and heart lumen formation (MacMullin & Jacobs, 2006; Medioni et al., 2008; E. Santiago-Martinez et al., 2008) the interactions between *slit* and integrins, slit and *sdc*, and *sdc* and integrins suggest that Slit/Robo signalling is more complex and it may require a greater signalling machinery composed of Integrin and Syndecan.

1.6 Integrins

Cells within tissues require two types of adhesion: direct cell-cell adhesion, primarily mediated by cadherins; and cell adhesion to the extracellular matrix, primarily mediated by integrins (R. O. Hynes, 2002). Integrins contribute to most, if not all, of the morphogenetic events that shape a developing organism (Bokel & Brown, 2002). Integrins are heterodimeric transmembrane receptors

composed of one α and one β subunit. These cell–extracellular matrix receptors appear to act as cellular sensors, where they constantly communicate with the surrounding ECM, and modulate cell behaviour accordingly (Stupack, 2007). Through various effector proteins, they connect to and regulate the actin cytoskeleton, controlling adhesion, cell growth, survival, migration, and differentiation (Stupack, 2007). Integrins have the ability to signal bidirectionally, meaning they can induce intracellular changes in response to extracellular cues (outside-in signalling) but they can also change their behaviour, such as their affinity for ligands, in response to intracellular changes (inside-out signalling) (Hughes, Oertli, Han, & Ginsberg, 2001; Legate, Wickstrom, & Fassler, 2009). Integrins are also essential for migration and certain types of cell behaviour, since the ability of a cell to form processes and migrate on a given substrate depends of the specific recognition by its integrin receptor (Bokel & Brown, 2002) and there is evidence that integrins are involved in the formation of the ECM to which they bind (Wu, 1997). Changes in cell adhesiveness in response to developmental cues are critical in cell migration and differentiation. Cell adhesion is controlled by modulating the binding properties of cell surface receptors and their ligands. In a number of cases it has been shown that integrin affinity for extracellular ligands is modulated by an intracellular mechanism (inside-out signalling), and that this modulation results in changes in cellular behaviour (M. D. Martin-Bermudo, Dunin-Borkowski, & Brown, 1998a).

Humans have at least eighteen α subunits and eight β subunits that can assemble into 24 different combinations that have overlapping ligand specificity and cell-type-specific expression patterns(R. O. Hynes, 2004)(R. O. Hynes, 2002). Furthermore there is functional redundancy between integrin dimers and subunits complicating the analysis of individual knockout phenotypes (Bokel & Brown, 2002). Model organisms such as *Drosophila* with fewer integrin subunits (five α and two β subunits) serve as practical developmental tools to test the importance of integrins (Brown, Gregory, & Martin-Bermudo, 2000).

The *Drosophila* integrins have been termed position-specific (PS) integrins, for their initially identified patterns of expression (Brown et al., 2000). The βPS1 *myospheroid* (*mys*) is the predominant β subunit in *Drosophila*. It is the dimerizing partner of three well characterized α subunits: αPS1 *multiple edematous wings* (*mew*) (Brower et al., 1995), αPS2 *inflated* (*if*) (Wilcox, DiAntonio, & Leptin, 1989), and αPS3 *scab* (*scb*) (Grotewiel, Beck, Wu, Zhu, & Davis, 1998; Stark et al., 1997). The other two α subunits αPS4 and αPS5 have not been characterized yet. The αPS4 gene lies downstream of αPS3, suggesting that it may rely on regulatory elements within the αPS3 gene. It is not known whether *scab* alleles affecting transcription affect both αPS3 and αPS4. Because of the high sequence similarity between αPS3, and αPS4 and αPS5, it is possible that βPS1 forms heterodimers with these α subunits as well (Brown et al., 2000). The second β subunit, βv, appears to be restricted in its expression to the endodermal cells of the gut (Yee & Hynes, 1993). Null mutations in the gene

encoding βv suggest it is not required for viability or fertility, and overall the mutant flies are normal in appearance. In the absence of both maternal and zygotic βPS1 the second β subunit can partially compensate for loss of βPS integrins in midgut formation. One study has identified αPS3 as a heterodimeric partner for βv (Devenport & Brown, 2004).

In the embryo the αPS1/βPS1 integrin is expressed in the epidermis and the endoderm (Leptin, Bogaert, Lehmann, & Wilcox, 1989), the αPS2/βPS1 integrin is expressed in the mesoderm. (Bogaert, Brown, & Wilcox, 1987) and the αPS3/βPS1 integrin is expressed in the visceral mesoderm. Throughout development αPS3/βPS1 is expressed in the amnioserosa, dorsal vessel, gut, salivary glands, midline cells of the ventral nerve cord and the mushroom body (Grotewiel et al., 1998; Stark et al., 1997). Both αPS1/βPS1 and αPS2/βPS1 are required for normal muscle development. Loss of αPS2/βPS1 causes embryonic lethality, its absence in the somatic muscles results in muscle detachment and in the visceral mesoderm it leads to gut defects (Brown, 1994). On the other hand, αPS1 (*mew*) mutants die as first instar larvae with defects in gut morphogenesis but no detachment in muscles. This exemplifies only one of the several adhesive and signalling roles during development. These integrins have been extensively studied in attachment of somatic and visceral muscles, morphogenesis of the gut and epidermis, and adhesion between the two surfaces of the wing blade (Brown et al., 2000). However there is very little known about the role of integrins in heart

morphogenesis. Because of the expression of the αPS3/βPS1 integrin in the heart and amnioserosa this integrin dimer will be the focus of this thesis.

Mutations in αPS3 cause a range of phenotypic strengths from embryonic lethal with dorsal holes (*scab* alleles) to adult viable with impaired learning (*volado* alleles) (Grotewiel et al., 1998; Stark et al., 1997)). Although the ligand for αPS3/βPS1 has not been well established phenotypic, genetic and sequence data suggest it could be a laminin-binding integrin (M. D. Martin-Bermudo, Alvarez-Garcia, & Brown, 1999; Stark et al., 1997). Several defects are seen in *scb* mutant embryos, all of which are shared with *mys* and some with *lanA* (Laminin A); among them are defects previously reported in *mys*, but not in *mew* (αPS1) or *if* (αPS2) mutations (Stark et al., 1997).

1.61 Integrins in the heart

In *Drosophila* the coordinated migration of the cardial cells towards the dorsal midline occurs in close proximity with the overlying ectoderm (Rugendorff et al., 1994). As such, it has been hypothesized that the migration of the cardial cells, leading edge, overlying ectoderm and the amnioserosa occur in a highly regulated manner, with cell adhesion and ECM molecules playing a major role in the proper migration towards the dorsal midline (Rugendorff et al., 1994).

In the nervous system integrins and integrin ligands interact genetically with *slit* to ensure proper axon guidance (Stevens & Jacobs, 2002). Decreased levels of Integrin function make axons more sensitive to changes in axon

guidance signalling. It was hypothesized that Integrin signalling or adhesion acts to increase the threshold for growth cones to respond to guidance signals (Stevens & Jacobs, 2002). In the *Drosophila* heart, Slit function may also include adhesion-related functions. This is supported by the phenotypes between *slit*, integrins and integrin ligands (Appendix 1, Fig.A1.2). The guidance role of Slit and its relationship with these adhesive forces was examined by Allison MacMullin and provided some of the basis for this thesis project.

Heart assembly defects have been previously described for βPS1 (*mys*), αPS3 Integrin (*scab*) and the integrin ligand Laminin (*lanA*) (Martin et al., 1999; M. D. Martin-Bermudo et al., 1999; Stark et al., 1997; Stark et al., 1997). Evidence suggests that in the heart, Slit signalling is dependent on adhesive signals from the αPS3/βPS1 integrin, since it has been shown that downstream Integrin linkers such as Talin and Integin Linked Kinase (ILK) also interact genetically with *slit* (Appendix 1 Fig. A1.3). In addition, *slit* was also found to interact genetically with other adhesion factors including ECM integrin ligands Laminin A and collagen type IV (*viking*) (Appendix 1, Fig. A1.4). interestingly, the cardiac defects observed in embryos lacking Integrin function are similar to those observed in embryos lacking Slit. The similarity between the heart phenotypes is suggestive of a role for Slit that may act with or in parallel with integrin activity. In addition, *scab* was found to have strong genetic interactions with *robo* and genes required for second messenger signalling downstream of Robo further supporting the notion that the two pathways converge.

The interaction observed between integrin genes and genes required for Slit/Robo signalling suggests that the two pathways intersect upon a common function. Integrins are key factors in cell migration and cell-matrix adhesion and are required for assembly of the heart. The defects in heart morphology observed when the Slit and the Integrin pathway were simultaneously altered such as delayed migration of cardial cells; cell clumping and midline crossing suggest that this function is an adhesive one. Based on this and since cardioblasts only express the αPS3/βPS1 Integrin dimer the objective of this thesis was to further explore the role of αPS3 in heart morphogenesis in the context of Slit and Robo signalling, focusing on adhesion and cell polarization. I hypothesize that αPS3 functions during heart assembly by affecting Slit/Robo signalling in the heart cells. To test this hypothesis I have established three specific aims:

1. Generate an antibody specific for αPS3 to help visualize Integrin localization in the heart cells.
2. Visualize Slit and Robo localization in the absence of the αPS3 integrin subunit.
3. Explore heart cell polarity in the absence of the αPS3 integrin subunit.

Chapter Two: METHODS

2.1 Fly Stocks

Fly stocks and crosses were maintained on sugar-salt-yeast agar medium at room temperature (21-23°C) (unless otherwise noted) in polypropylene shell vials (Fisher Scientific, AS519) or 16 x 100 mm glass culture tubes (Fisher Scientific, 14 961 29) plugged with rayon rope (Fisher Scientific, 12 640 41). Flies were transferred to fresh vials every 15 days and adults were cleared from vials one week after transfer.

Mutant strains *scb*^{2}, *scb*^{01288}, *sli*^{2}, *robo*^{1}, were obtained from the Bloomington Stock Centre as well as the muscle specific driver *dMef-GAL4* and the ubiquitous driver *daughterless-GAL4*, *UAS-scb* RNAi (100949) and *UAS-mys* RNAi (103704) fly stocks were obtained from the Vienna Stock Centre, and *UAS-par-6::GFP* was provided by Tony Harris (David, Tishkina, & Harris,). The *lacZ* enhancer trap line B2-3-20 was provided by E. Bier (Bier et al., 1989). *UAS-scab* and *UAS-scabΔC* were created by Allison MacMullin. Single mutant lethal lines were maintained over a balancer chromosome containing a P[engrailed-*lacZ*] for 2nd chromosome mutations and a TM3,Sb balancer for 3rd chromosome mutations. Homozygous mutants were identified by the lack of β-Galactosidase labelling. The following table is a detailed list of mutant stocks used in this thesis.

Table 2.1 Mutations and transgenic lines used

Stock	Gene	Features	Function	Source	Reference
yw; scab^{2}/Cyo[enLacZ]	*scab*	Loss of function; EMS No detectable RNA transcrip	αPS3 subunit; cell adhesion, signal transduction	Bloomington Stock Centre	Tearle and Nusslein-Volhard 1987; Stark *et al*, 1997.
yw; scab^{10288}/Cyo[enLacZ]	*scab*	Hypomorph; P-element in first intron of long isoform	αPS3 subunit; cell adhesion, signal transduction	Bloomington Stock Centre	Stark *et al*, 1997;FlyBase
yw; slit^{2}/Cyo[enlacZ]	*slit*	Loss of function; EMS	Attractive/repulsive cue; Binds Robo	Bloomington Stock Centre	Rothberg *et al*, 1988; Battye *et al*, 1999; Kidd *et al*; 1999.
yw; robo1^{1}/Cyo[enlacZ]	*robo1*	Amorph; EMS	Robo1 receptor; Binds Slit	G. Tear	Seeger *et al*, 1993; Kidd *et al*, 1998
yw; UAS scab	*scab*	Full length *scab* under control of UAS promoter	αPS3 subunit; cell adhesion, signal transduction	R. Jacobs	This thesis
UAS scabΔC/Y; +; +	*scab*	Cytoplasmic deletion in *scab*	αPS3 subunit; increased cell adhesion and reduced signal transduction	R. Jacobs	This thesis

2.2 Embryo collection and fixation

Adult flies were crossed in well ventilated plastic beakers capped with petri dishes containing apple juice agar and yeast paste for feeding. Embryos were collected on the apple juice agar and aged at room temperature (21-23°C) followed by incubation at 18°C to stage embryos at late (stage 16-17) embryogenesis. For RNAi experiments, embryos were collected every 2-4 hours at room temperature (21-23°C) followed by incubation at 29°C for 12 hours to stage embryos at late embryogenesis. Collection and incubation times were modified according to the genotype. Plates were kept at 4°C to arrest development before fixation for periods no longer than 72 hours after egg-laying. Prior to fixation or incubation, embryos kept at 4°C were placed at room temperature to allow for microtubule repolymerisation and to resume proper morphology. Embryos were dechorionated in 50% bleach in ddH_2O for 4-5 minutes, collected in nytex sieves and incubated in 3.7% formaldehyde in 1X phosphate buffered saline (PBS pH 7.4) and heptane (final volume of 10 mL) on a rotator for 25 minutes. Embryos were cracked out of their vitelline membrane in 100% methanol. Embryos were washed several times with 100% methanol to remove traces of fixative and heptane and stored at 4°C until use.

2.3 Immunohistochemistry

2.31 Immunolabelling

Prior to immunolabelling, embryos were washed 5 times in 0.1% PBT (0.1% Triton-X 100 or Tween 20 in 1XPBS (137mM NaCl, 2.7mM KCl, 4.3mM Na2HPO4, 1.47mM KH2PO4 pH 7.4)) and allowed to rehydrate for 20 minutes on a rotator in 0.1% PBT at room temperature. Embryos were blocked in 10% normal goat serum (NGS) (final volume of approx. 150 µl) on a shaker for 30 minutes. Primary antibody was added at the appropriate dilution and incubated overnight on a shaker at 4°C. Embryos were washed in 0.1% PBT for 4-8 hours with periodic changes every 30 minutes to an hour. Embryos were re-blocked in 10% NGS for 30 minutes and incubated with secondary antibody at the appropriate dilution for 2 hours on a shaker at room temperature. Embryos labelled with a fluorescent secondary antibody were protected from photobleaching by using tinfoil. Embryos were washed overnight in 0.1% PBT on a rotator at 4°C. The next day after 3-5 washes in 0.1% PBT at room temperature, fluorescently labelled embryos were stored in 70% glycerol at 4°C. For double labelled embryos the addition of primary and secondary antibody pairs was sequential, repeating the process after the overnight wash. Embryos labelled using a biotinylated secondary antibody (Vector Laboratories) were incubated for 1 hour in Vector Laboratories Elite ABC (Vector Laboratories, PK-6100) (2 µl each of solution A and B in 100 µl 0.1% PBT per reaction). Embryos were then washed 5 times with 0.1% PBT and the peroxidase reaction started by

the addition of 0.03% hydrogen peroxide to embryo mixture containing 3,3-Diaminobenzidine Tetra hydrochloride (DAB,Gibco-BRL). Embryos were washed with 0.1% PBT 5 times to remove all traces of DAB. Embryos were gradually dehydrated in ethanol (50, 70, 90, 95% ethanol in ddH_2O, and 100% ethanol) and stored at room temperature in methyl salicylate (Fisher Scientific, O3695 500).

2.32 Antibodies

Primary and secondary antibodies described in Table 2.2 and Table 2.3.

2.4 Mounting and Imaging

Fluorescently labelled embryos were mounted in 70% glycerol on microscope slides using a three coverslip method. Embryos were deposited between two adjacent coverslips (approx. 5 mm apart) and covered by a third. Embryos were mounted and all coverslips were sealed with nail polish at least 1 hour prior to visualization by confocal microscopy using a Leica SP5 microscope. Images are projections of 3-5 sections (1µm thick). Embryos labelled using a biotinylated secondary antibody were mounted in D.P.X. neutral mounting medium (Sigma-Aldrich, 317616) and visualized using Zeiss Axioskop microscope. All images were processed using Image J, OpenLab and Adobe Photoshop.

Table 2.2: Primary antibodies used for immunohistochemistry

Primary Antibody	Type	Source	Dilution	Notes
anti-β-galactosidase	Chicken Polyclonal	Mihaela Georgescu	1:150	*Recognizes β-galactosidase expressed by the LacZ gene. Used to visualize the cardial LacZ enhancer trap B2-3-20 and LacZ marked balancers.
anti-Scab	Rabbit Polyclonal	Luz de Lourdes Vazquez Paz	1:600	*Serum. Recognizes overexpressed αPS3. Too weak to pick-up endogenous levels of the integrin..
Anti-dMef2	Rabbit Polyclonal	Jessica Vanderploeg	1:50000	*Serum. Recognizes *Drosophila* *Myocyte enhancer factor 2. Used to visualize muscle cell nuclei including the heart.
anti-GFP	Rabbit Polyclonal	Invitrogen Molecular Probes A6455	1:600	*Recognizes green fluorescent protein and yellow fluorescent protein. Very strong antibody. Some background.
C555.6D	Mouse Monoclonal	Developmental Studies Hybridoma Bank	1:30	*Recognizes Slit protein, C-terminal portion. At early it stages it surrounds the cell. At stages 16-17 it is secreted to the lumen of the heart.
13C9	Mouse Monoclonal	Developmental Studies Hybridoma Bank	1:30	*Recognizes Robo. At stages 16-17 it decorates the lumen of the heart. Best on fresh non MeOH stored embryos and best with Tween20 (0.1% Tween-20 in 1XPBS).
EC11	Mouse Monoclonal	Developmental Studies Hybridoma Bank	1:30	*Recognizes Pericardin, it decorates the ECM surrounding the pericardial cells and the cardial cells of the heart. Used as a basal polarity marker.
3A9	Mouse Monoclonal	Developmental Studies Hybridoma Bank	1:30	*Recognizes αSpectrin, it decorates the lateral membrane of almost all cell types including the cardial cells. Used as a lateral marker.
4F3	Mouse Monoclonal	Developmental Studies Hybridoma Bank	1:30	*Recognizes Discs large (Dlg), it decorates the basal-lateral membrane of cells. Used as a lateral polarity marker. In the heart Dlg is seen in the apical-lateral membrane.
6G11	Mouse Monoclonal	Developmental Studies Hybridoma Bank	1:10	*Recognizes βPS1 integrin (Mys). It decorates the Integrin heterodimer on the cell surface. At stages 16-17 Integrins are found in the apical surface of the cardial cells.

Table 2.3: Secondary antibodies used for immunohistochemistry

Secondary Antibody	Type	Source	Dilution	Notes
Goat anti-Mouse Alexa Fluor 488	Fluorescent	Molecular Probes A11001	1:150	*Emission colour green. Seems to cross-react with chicken 2° antibodies. Use first in sequential staining protocol.
Goat anti-Mouse Alexa Fluor 594	Fluorescent	Molecular Probes	1:150	*Emission colour red. Seems to cross-react with chicken 2° antibodies. Use first in sequential staining protocol.
Goat anti-Rabbit Alexa Fluor 488	Fluorescent	Molecular Probes	1:150	*Emission colour green. Does not cross-react with other 2° antibodies. Can be used in simultaneous double labelling protocols including mouse antibodies.
Goat anti-Rabbit Alexa Fluor 594	Fluorescent	Molecular Probes	1:150	*Emission colour red. Does not cross-react with other 2° antibodies. Can be used in simultaneous double labelling protocols including mouse antibodies.
Goat anti-Chicken Alexa Fluor 488	Fluorescent	Molecular Probes	1:150	*Emission colour green. Does not cross-react with other 2° antibodies. Can be used in simultaneous double labelling protocols except mouse antibodies.
Goat anti-Chicken Alexa Fluor 594	Fluorescent	Molecular Probes	1:150	*Emission colour red. Does not cross-react with other 2° antibodies. Can be used in simultaneous double labelling protocols except mouse antibodies.
Goat anti-Chicken BIO	Biotinylated	Vector Laboratories	1:150	*For use with ABC Kit and DAB. Not for Western Blotting
Goat anti-Rabbit BIO	Biotinylated	Vector Laboratories	1:150	*For use with ABC Kit and DAB. Not for Western Blotting

2.5 Rabbit Polyclonal anti-αPS3 Antibody Generation

2.51 Preparation of His tagged αPS3 construct

A region containing the first 1,665 base pairs of the *scab* gene was amplified by PCR using the following primer sequences: 5' AAA **GAA TTC** GAT GGT GGG GCA AGA TCGT 3' forward primer and 5' CTC **GAA TTC** ATG GCT AGT TCC TGT TCT TG 3' reverse primer. Restriction site EcoRI was incorporated into the primers for cloning purposes. The PCR product was directly cloned into pCR2.1 vector using the TA cloning Kit (Invitrogen, 45 0046), transformed into Subcloning Efficiency DH5α Chemically Competent *E. Coli* (Invitrogen, 18265 017) and screened for white positive transformants on selective plates containing X-gal. Once a positive *scab* pCR2.1 transformant was confirmed, the *scab* fragment was subcloned into pET29b vector using the EcoRI restriction sites. The *scab* pET29b plasmid was then transformed into One Shot BL21 Chemically Competent *E. coli* (Invitrogen, C6000 03) for protein induction.

2.52 αPS3 His Tagged Protein Induction and Purification

An inoculated culture of *scab* pET29b was grown overnight for 16 hours at 37°C on a shaker. The overnight culture was used to inoculate 1L of LB containing Kanamycin (final concentration of 3ug/ml) to a final OD_{600}~0.05. After inoculation the culture was incubated at 37°C on a shaker until the OD_{600} ~0.5 was reached. The culture was then induced with 0.4mM of IPTG (Isopropylthio-

beta-D-galactosidase) (Invitrogen, 15529019) and allowed to grow for an additional 4 hours at 26°C with shaking. The cells were then harvested by centrifugation at 10,000 rpm for 10 minutes at 4°C and stored at -20°C until purification of the αPS3 His tagged protein.

The αPS3 His tagged protein was purified using a denaturing method due to sequestering of the protein in inclusion bodies during the induction phase. For this method the cells were thawed on ice and resuspended in 25ml of ice cold 1XPBS pH 7.4 per 250ml of culture volume. The inclusion bodies were collected by centrifugation at 5,000 x g for 15 min at 4°C. The pellet was resuspended in 2ml cold M-SSB buffer (2% SDS, 0.2M β-mercaptoethanol, 50mM Tris-HCl pH 6.8, 1mM Na-Or, 1mM Na-F) containing a complete EDTA-free protease inhibitor (Roche Diagnostics, 1873580) and 18ml Buffer B (100mM NaH_2PO_4, 10mM Tris-HCl, 8M urea, pH 8.0) per 250ml culture volume. The cells were sonicated using a Sonifier Cell Disruptor 350 (Branson Sonic Power serial no. 8D60019A) on ice for 5 minutes with 30 second breaks between each minute. Insoluble material was removed by centrifugation at 5,000 x g for 15 minutes at 4°C and the supernatant was stored at 4°C for purification by affinity chromatography.

Large scale purification of the αPS3 His tagged protein was done by combining the batch purification method and the column chromatography method. To prepare for protein purification using batch adsorption, 2ml of His-Select Nickel Affinity Gel (Sigma-Aldrich P6611) suspension was added to a

centrifuge tube and pelleted by centrifugation at 5,000 x g for 5 minutes. The gel was then washed with 2 volumes of sterile distilled water, equilibrated with 10 volumes of equilibration/wash buffer (50mM sodium phosphate, 0.5M NaCl, 8M urea, pH 8.0) with centrifugation at 5,000 x g for 5 minutes between each wash. Once the last of the equilibration buffer was removed, the cell extract was added to the affinity gel and allowed to bind for 2 hours at 4°C on an orbital shaker. Once the binding was complete the affinity gel was transferred to a column and was allowed to settle under gravity flow. The column was then washed with 10 volumes of equilibration/wash buffer. The His tagged protein was then eluted from the column with 5 volumes of elution buffer (50mM sodium phosphate, 100mM NaCl, 8M urea, 250 mM imidazole, pH8.0).

The affinity purified αPS3-His fusion protein was dialyzed in PBS for 5 hours at room temperature (21-23°C) to prevent protein aggregation. The Bradford Assay (Bradford, 1976) was used to determine final protein concentration and SDS-PAGE analysis was used to confirm protein integrity.

2.53 Immunization

Antiserum was prepared by mixing purified αPS3 His tagged protein (final concentration of 100ug/ml) in PBS with Freund's complete adjuvant (CFA) until a homogenous suspension was obtained. The mixture was delivered through intramuscular injection into 2 New Zealand white rabbits at 3 different sites where each site received 0.3 ml. After prime immunization, follow up booster shots were

given to each rabbit every 21 days using incomplete Freund's adjuvant instead of CFA. Before each injection an ear bleed of 5ml from each rabbit was taken. To prepare the sera, the bleeds were incubated in a water bath at 37°C for one hour to allow maximum clotting and then placed at 4°C overnight. The next day the serum was centrifuged at 10,000 rpm at 4°C and the supernatant was collected. Sodium azide was added to prevent bacterial contamination to a final concentration of 0.01% and the sera was stored at -80°C.

2.6 Preparation of Crude Protein Lysate from *Drosophila* Tissue

2.61 Protein Lysate Extraction from *Drosophila* Embryos

Embryos were collected every two hours at room temperature (21-23°C) followed by incubation at 29°C for 12 hours to stage embryos at late embryogenesis. Embryos were harvested from apple juice agar plates onto nytex sieves using distilled water. Collected tissue was homogenized on ice in cold SDS-Sample Buffer (2% SDS, 10% glycerol, 5% β-mercaptoethanol, 60mM Tris-HCl pH 6.8,1mM Na-F, 1mM Na-VO_4) containing a complete EDTA free protease inhibitor (Roche Diagnostics, 1873580) using a volume of ~100µl per day collection. Embryos were ground 2 times and centrifuged for 10 minutes at 10,000 rpm at 4°C after each homogenization. The supernatant was collected and final protein concentration was determined using the Bradford Assay (Bradford, 1976). Aliquoted samples were boiled at 95°C for 5 min, vortexed and

stored at -80°C until use. Before loading onto SDS-PAGE gel 2µl of bromophenol blue were added to sample.

2.62 Protein Lysate Extraction from *Drosophila* Heads

Adult flies were flash frozen in liquid nitrogen and decapitated by vigorous vortexing. Heads were separated and counted on a nytex sieve kept over ice and transferred into micocentrifuge tubes using a brush. Collected tissue was homogenized on ice in cold RIPA lysis buffer (150mM NaCl, 1% NP-40, 0.5% deoxycholic acid, 0.1% SDS, 50mM Tris-HCl pH 8.0) containing a complete EDTA free protease inhibitor (Roche Diagnostics, 1873580). Extraction was done with a volume of 1µl per head (but no less than 30µl). Heads were ground 3 times and centrifuged for 10 minutes at 10,000 rpm at 4°C after each homogenization. The supernatant was collected and final protein concentration was determined using the Bradford Assay (Bradford, 1976). Samples were aliquoted and stored at -80°C until use.

2.7 Heat Shock

To verify the transgenic expression of full-length Scab protein, 1-2 days old adult flies *w-;HSP70-GAL4;UAS-scb* or *w-;CyO;UAS-scb* were subjected to dry heat shock at 37°C for 1 hour. Flies were allowed to recover at room temperature for 1 hour. The heat shock and recovery treatments were repeated 3 times. A dry heat shock method using a sandbox warmed to 37°C was used instead of a water bath heat shock to minimize fly loss due to condensation inside

the glass tubes. Flies were transferred to a microcentrifuge tube and stored at -80°C until use. Protein lysate from the adult heads was collected as outlined above.

2.8 Western Blot Analysis

Crude protein samples containing 50-60ug of protein were mixed with 5X SDS loading buffer (2% SDS, 10% glycerol, 100mM DTT, 60mM Tris pH8.0, 0.01% bromophenol blue, 5% 2-mercaptoethanol), boiled for 5 minutes at 95°C and centrifuged at 10,000 rpm for 10 min at 4°C. The protein samples were loaded onto a 10% SDS-polyacrylamide gel and run at 100V for 90 minutes. After electrophoresis the protein was transferred to a PVDF membrane (Pall Life Sciences, P/N 66543) at 100V for 1 hour at 4°C. Following the transfer, the membrane was blocked in 5% skim milk in 1X PBS-T (0.1% Tween 20 in 1X PBS) for 1 hour at room temperature (21-23°C). The membrane was incubated in a 1:100,000 dilution of the rabbit polyclonal anti-αPS3 serum in 3% skim milk in 1X PBS-T overnight at 4°C. The membrane was then washed 3 times with wash buffer (1X PBS-T) to remove any unbound primary antibody. The membrane was incubated in a 1:5,000 dilution of horseradish peroxidise conjugated secondary antibody for 1 hour at room temperature. The membrane was washed 3 times with wash buffer to remove any unbound secondary antibody and prepared for developing using Pierce ECL Western Blotting Substrate (Thermo Scientific PI32106). and Amersham Hyperfilm ECL (GE Healthcare, 28906838).

2.9 RNAi Lethality

To determine the percentage of lethality caused by the overexpression of the dsRNA constructs, *UAS-scb* RNAi (100949) and *UAS-mys* RNAi (103704) were crossed to *da-GAL4* and *dMef-GAL4*. Embryos were collected on apple juice agar plates for four hours at room temperature (21-23°C). A total of 120 embryos were aligned on a fresh apple juice agar plate and incubated at 29°C for 24-48 hours. The number of hatched embryos was recorded. Embryos that failed to hatch were placed on a microscope slide covered in double-sided tape. Using forceps embryos were unrolled from their chorion layer. The number of unfertilized embryos and fertilized unhatched embryos was recorded and the % viability was calculated using the following formula:

$$\frac{\text{number of fertilized unhatched embryos}}{\text{total number of embryos} - \text{number of unfertilized embryos}} \text{ X } 100 = \%\ \text{Lethality}$$

2.10 *UAS-scb* Rescue of scb^2 Null Embryos

The heart mutant phenotype of homozygous null embryos is partially restored by overexpression of *UAS-scb* by *dMef-GAL4*. w-;scb^2/$CyO_{[en\text{-}lacZ]}$;UAS-scb flies were crossed to w-;scb^2/$CyO_{[en\text{-}lacZ]}$;*dMef-GAL4, B2-3-20* flies. Embryos were collected on apple juice agar plates for 4 hours at room temperature (21-23°C) and staged at late embryogenesis. Embryos were collected, immunolabelled, mounted and imaged as previously described. Restoration of the heart phenotype was scored as described below.

2.11 Scoring of Heart Mutant Phenotypes

Scoring of the severity of heart phenotype was adapted from MacMullin and Jacobs (MacMullin & Jacobs, 2006). Abnormalities were grouped into four categories, since *scab* phenotypes are very different from those caused by *slit*, abnormalities were grouped into new categories. Categories created were Irregular migration, Cell clumping, Midline crossings and Other. Under the Other category several abnormalities are grouped such as twists (contralaterally placed cardial cell nuclei), gaps (cardial cells missing from a row of migrating cardial cells) and delays (cardial cells more laterally placed than wild type at that stage, effects due to dorsal closure also fall under this). Abnormalities were recorded in 20 embryos staged at late embryogenesis (stages 16-17) giving them a score of 0 for the absence of the abnormality and a score of 1 for the presence of the abnormality up to 4 per embryo. Embryos were then ranked on an ordinal scale from 0 to 4 assigning a 1 for each category that has a score of more than 0 for an abnormality. Severity was calculated as the averaged number of defects per embryo per category. Penetrance is the fraction of embryos with two or more abnormalities.

Chapter Three: RESULTS

3.1 Generation of a polyclonal antibody to visualize Integrin localization in the *Drosophila* heart

In order to explore integrin behavior during normal and irregular heart development, it was first necessary to generate an antibody specific to αPS3. *scab* expression has been previously reported in the salivary gland, trachea, midgut, dorsal vessel, midline of the ventral nerve cord, and the amnioserosa (Stark et al., 1997) however this was assayed by RNA in-situ hybridization. Other assays using an antiserum made against the C-terminus of the protein found αPS3 to be concentrated in the mushroom body (Grotewiel et al., 1998) however this antiserum is no longer available.

Antiserum against the N-terminus of the αPS3 integrin was generated in rabbits using a His-tagged protein. Following antibody generation and serum preparation, the antibody was tested on Western blots. Pre-immune controls show no staining.

αPS3 protein production was induced after heat shock (HS) in *w-;HSP70-GAL4;UAS-scb* adult flies and *w-;CyO;UAS-scb* used as an internal negative control. Immunoblotting was performed on extracts from head tissue without (0h) or after 3h HS. Western blots containing ~60μg of protein per lane were incubated with the serum generated against αPS3 (Appendix 2 Fig.A2.2 A). A

~125kDa band corresponding to the over-expressed protein (*w-;HSP70-GAL4;UAS-scb* 3h HS) can be seen in comparison to the negative control without HS (*w-;HSP70-GAL4;UAS-scb* 0h HS) and the internal negative controls (*w-;CyO;UAS-scb* 3h and 0h HS). However endogenous αPS3 was not detected. The predicted molecular weight of αPS3 is approximately 124kDa therefore there is little reason to believe the 150kDa band detected belongs to endogenous αPS3. There is only one report of αPS3 being detected by immunoblot and this protein ran at approx. 135kDa (Grotewiel et al., 1998).

In a similar experiment, Western blots containing different concentrations of protein lysate from flies expressing endogenous levels of αPS3 were probed with the antiserum (using extracts of flies over-expressing αPS3 with a ubiquitous driver as a positive control). Once again, the antiserum recognized the over-expressed protein (~125kDa) but failed to recognize the endogenous protein and the unidentified band (~150kDa) was recognized once more suggesting cross-reaction or unspecific binding (Appendix 2 Fig.A2.2 B)

I also performed immunohistochemical analysis since some antibodies are known to work better in tissue versus immunoblotting and vice versa. After multiple dilutions and different buffers (PBT with Tween-20 versus Triton-X 100) immunohistochemistry revealed little specificity for the endogenous αPS3 in tissue (Appendix 2 Fig.A2.2 C)

3.2 Altered Integrin expression results in heart assembly defects

The integrin αPS3/βPS1 is the only dimer expressed in the heart (Stark et al., 1997). Heart assembly defects have been previously described in embryos lacking the αPS3 integrin (*scb*). Shown here is a more detailed analysis of the αPS3 requirement for heart formation.

Using the B2-3-20 enhancer trap to visualize the cardial cells and LacZ marked balancers, embryos homozygous for a null allele of *scab* (*scb2)* (Stark et al., 1997; Tearle & Nusslein-Volhard, 1987) a hypomorph of scab (*scab01288*) (Tweedie et al., 2009), and embryos expressing *scab* transgenes *UAS-scab* and *UAS-scabΔC* (MacMullin unpublished) were assayed for heart developmental defects (Fig.3.1). The migration of the cardial and pericardial cells towards the dorsal midline occurs in close proximity to the dorsal ectoderm. Mutants that have a dorsal closure defect will show heart defects as a secondary effect (Rugendorff et al., 1994). *scab* mutants were identified by its dorsal closure phenotype (Tearle & Nusslein-Volhard, 1987). The assessment and scoring of *scb2* mutant embryos proved difficult because the lack of proper dorsal closure in these mutants causes the gut of the developed embryo to protrude out of the dorsal hole pushing the cardial cells outward thus making the heart defects much more pronounced. For this reason, the delays in heart closure were grouped under the "Other" category as its appearance cannot be uncoupled from a dorsal closure effect. The cardial cells in the posterior portion of the heart manage to reach the midline thus most of the analyses were carried out in this area of the dorsal vessel known as the

heart proper. The hypomorphic allele *scb01288* has a less pronounced dorsal closure defect allowing cells to migrate further making some of the later occurring phenotypes more apparent thus giving it a higher severity score (see Fig.3.1C and Table 3.1). There was a wide range of assembly defects used to assess the severity of the heart phenotypes. The scoring method was adapted from MacMullin and Jacobs (MacMullin & Jacobs, 2006) because some of the phenotypes were largely based of *slit* mutant heart defects. Common *scab* mutant phenotypes include delayed migration (asterisk), gaps, and blisters in the heart, and twists, or midline crossing of cardial cell nuclei. Cell migration and final assembly of the heart vessel is slower and disorganized compared to wild type. Embryos mutant for *scab* have breaks in the continuity of the cardial cells during migration (Figs. 3.1B, C, G-I) and nuclei may cross the midline, and irregular cell clumps are also seen (arrowhead Fig.3.1G). The range of phenotypes varies in the severity; however the heart phenotype, independent of dorsal closure, in *scb2* mutants is 85% penetrant as assessed by our scoring method (Table 3.1)

To further examine the role of αPS3 in heart morphogenesis *UAS-scab* was over-expressed using the muscle specific driver *dMef-GAL4* in wild type and *scab* mutant backgrounds. Embryos over-expressing αPS3 show delays in cell migration (asterisk Fig.3.1D) (not obvious in our scoring method due to the grouping of delayed closure under the "Other" category) and some other mild defects (Table 3.1). αPS3 over-expression in *scb2* was able to partially restore

migration (Table 3.1) however overall morphology of the embryo could not be restored due to dorsal closure effects (Figs.3.1E-F).

3.21 Embryos expressing a cytoplasmically truncated αPS3 Integrin have severe perturbations in heart development

Removing the C-terminal of αPS3 should increase its ligand affinity (M. D. Martin-Bermudo, Dunin-Borkowski, & Brown, 1998b) allowing to explore the role of adhesion in heart morphogenesis. A C-terminal truncated version of the αPS3 integrin was expressed in heart and muscle cells using the *dMef-GAL4* driver in a wild-type and in a *scb2* mutant background. Over-expression of this transgene causes embryonic lethality in a wild type background and it is not able to rescue *scb2* lethality (Appendix 2 Table A2.1 and A2.2). *UAS-scabΔC;;dMef-GAL4, B2-3-20* embryos exhibit a dominant effect in cell migration seen as delayed and irregular migration of the heart cells (Fig. 3.1H and Table 3.1) suggestive of a stronger adhesive interaction with the matrix substrate during migration. Those cardial cells that reach the midline form a shorter heart due to severe cell clumping (Fig.3.1G). Furthermore, expression of the cytoplasmically truncated αPS3 Integrin partially rescues the *scb2* phenotype (Fig.3.1I). This suggests a role for adhesion perhaps independent of integrin signalling in heart morphogenesis.

Figure 3.1: Altered αPS3 expression phenotypes in the *Drosophila* heart

Stage 17 embryos homozygous for a null allele of *scab* (*scb2*) have severe heart development defects [B] when compared to wild type embryonic heart development [A]. Embryos homozygous mutant for a hypomorphic allele of *scab* (*scb01288*) also fail to have proper heart development [C] however they show milder heart and dorsal closure defects (arrow). Delays in heart closure (asterisk) are common defects observed in embryos lacking *scab* mutants along with irregular cell migration, where the rows of cells fail to be smoothly aligned. Other defects like twists or misplaced cardial cells (i.e. clumping and ectopic cells) are also seen in mutant embryos. Over-expression of αPS3 causes small delays in heart closure (asterisk) [D] and its expression in a *scb2* background partially restores the cell migration phenotypes observed with the null mutation [E-F]. Over-expression of a cytoplasmically truncated form of αPS3 (*scbΔC*) has a dominant effect on heart assembly. Embryos expressing this transgene have a wide range of phenotypes. Shown are the most commonly observed phenotypes: shorter hearts with severe cell clumping (arrowhead) [G] and severe irregularities in cell migration with delayed heart closure (asterisk) [H]. Over-expression in a *scb2* background partially restores heart assembly, however dorsal delays can still be observed (asterisk) [I] as well as some cell clumping and irregular cell migration. In all panels, cardial cells are labelled using anti-β-galactosidase to detect the B2-3-20 cardial cell enhancer trap. Anterior is to the top.

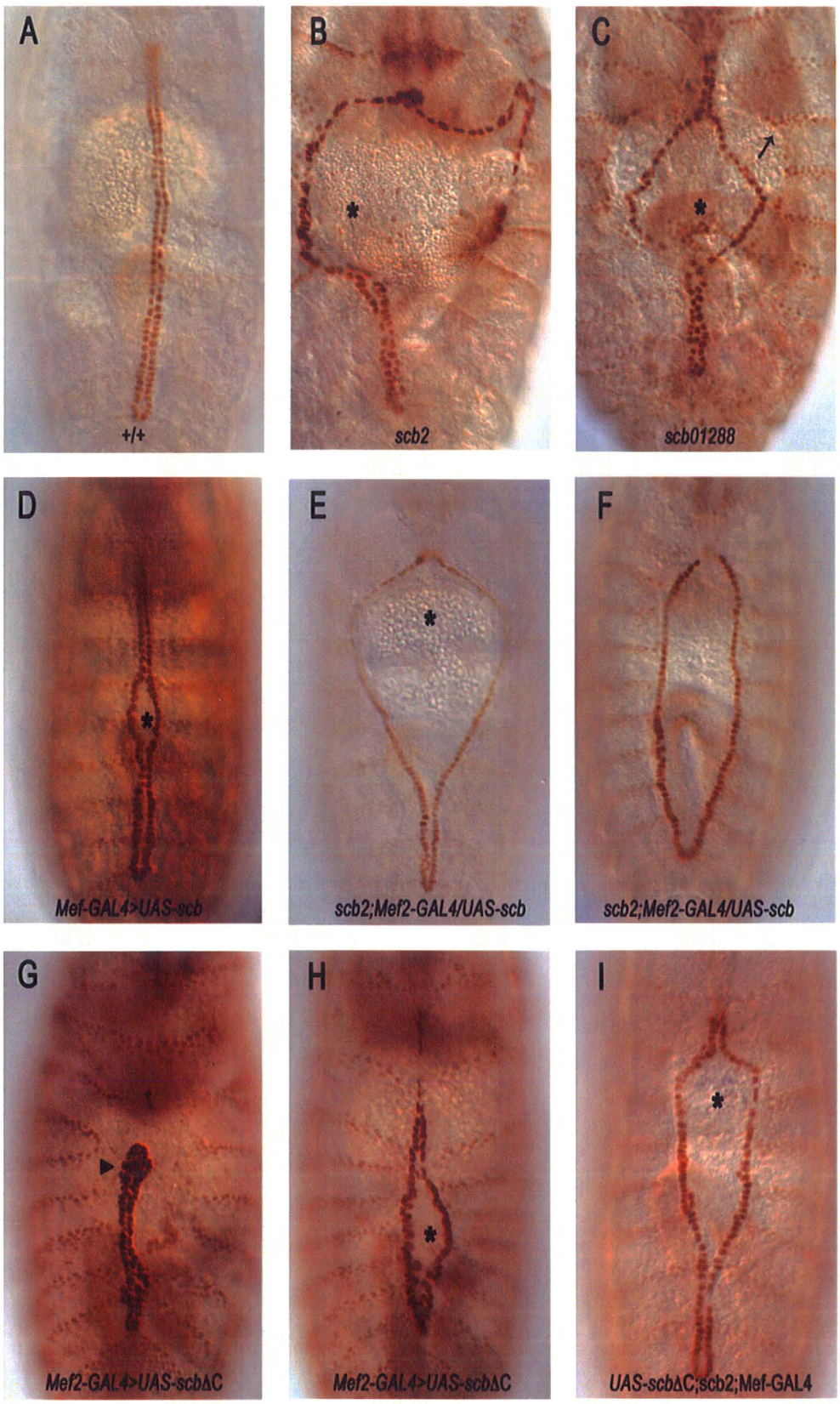
A
+/+
B
scb2
C
scb01288
D
Mef-GAL4>UAS-scb
E
scb2;Mef2-GAL4/UAS-scb
F
scb2;Mef2-GAL4/UAS-scb
G
Mef2-GAL4>UAS-scbΔC
H
Mef2-GAL4>UAS-scbΔC
I
UAS-scbΔC;scb2;Mef-GAL4

3.3 αPS3 is required for the formation of the heart lumen

Electron microscope transverse sections of wild type and *scab* mutant embryos (stage 17) reveal a requirement of αPS3 for lumen formation. By stage 17, the cardial cells (*c*) of wild type embryos have made contact and developed an apical lumen (arrow Fig 3.2A). In contrast, the cardioblasts of *scab* mutants that have made contact by stage 17, have an extensive area of apical surface adhesion and fail to develop a lumen (Fig.3.2B). Embryos expressing the C-terminal truncated version of αPS3 have a smaller and irregular heart lumen (Fig.3.2C).

3.4 Integrins are required for Slit and Robo apicalization

It has been shown that Slit/Robo signaling is also required for heart lumen formation (MacMullin & Jacobs, 2006; Medioni et al., 2008; E. Santiago-Martinez et al., 2008). Previous research by Allison MacMullin (MacMullin & Jacobs, 2006) showed heart assembly is severely compromised when both *slit* and *scab* expression is reduced. Such a strong interaction between *scab* and *slit* is suggestive of a role for Slit acting with or in parallel with Integrin activity. Are Slit and Robo affected in the absence of αPS3? In order to address this I used immunohistochemistry and confocal microscopy.

Using anti-Beta-galactosidase to detect the B2-3-20 cardial cell enhancer trap to visualize the cardioblasts and monoclonal antibodies I examined the localization of Slit and Robo protein in the absence of the αPS3 integrin and in

wild type embryos. Wild type expression of Robo and Slit was first detected during stages 13-14 of embryogenesis surrounding the cardioblasts. Apicalization of both proteins was first observed at stage 16 of embryogenesis when the cardioblasts touch their contralateral partners followed by a strong accumulation in the lumen of the heart by stage 17 (Fig. 3.3A and B). In stage 17 wild type embryos, the monoclonal antibody against Robo decorates the apical side of cardial cells, alary muscles (asterisks) and pericardial cells (not seen in these images). Slit is seen in mainly in the apical surface of the lumen with some residual signal around the cardioblasts. In embryos homozygous for *scb2*, apicalization of Robo and Slit is incomplete as observed by the persistence of a lateral signal between cardioblasts (arrows Fig. 3.3C and D), this phenotype was also observed in the hypomorphic allele *scb10288* (Appendix 2 Fig.A2.1). In addition, *scab* mutant embryos show reduced levels of Robo (Fig. 3.2C) and Slit (Fig. 3.2D) as compared to wild type. Together these data support a role for integrins in Slit and Robo localization and concentration in the heart lumen.

Figure 3.2: αPS3 is required for lumen formation

[A] At stage 17, the wild type heart has a well developed lumen (arrow) between the contralateral cardioblast cells (*c*). [A] In embryos mutant for *scab*, those cardial cells that do meet at the midline do not form a lumen. [C] In embryos over-expressing the cytoplasmically truncated form of αPS3 the lumen is irregular and small (arrow). Removal of the carboxyl terminal of αPS3 is postulated to shift the integrin to a high affinity for extracellular ligands. Sectioning and electron microscopy performed by Dr. Roger Jacobs.

c - cardial cells

e -ectoderm

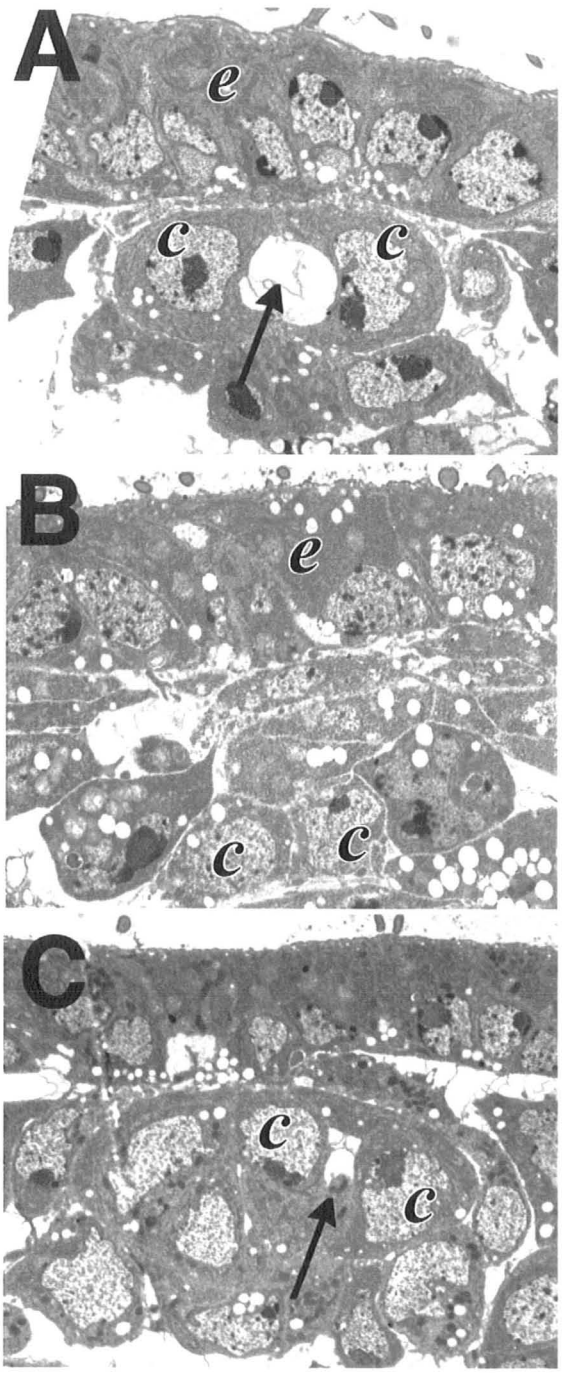
A
e
c
c
B
e
c
c
C
c
c

Figure 3.3: αPS3 is required for Slit and Robo concentration in the lumen

In wild type embryos Robo [A] and Slit [B] accumulate apically in the lumen where little lateral signal is observed. In contrast, *scb2* mutant embryos reveal lateral accumulation of Robo and Slit between the cardioblasts in the absence of the aPS3 integrin (arrows) [C-D]. A reduction in signal of Robo [C] and Slit [D] as compared to their wild type counterparts is observed (insets at same gain as control) suggestive of a role for integrins in accumulating Slit and Robo in the apical domain of the cardial cells. Dorsal view of stage 16-17 wild type [A-B] and *scb2* mutant [C-D] embryos immunolabelled using anti-β-galactosidase to detect the B2-3-20 cardial cell enhancer trap (green) and MAb to detect Slit and Robo (red) imaged using confocal microscopy. Because of the heart closure defects only the posterior of the heart is seen (anterior to the left). Calibration: 10μm

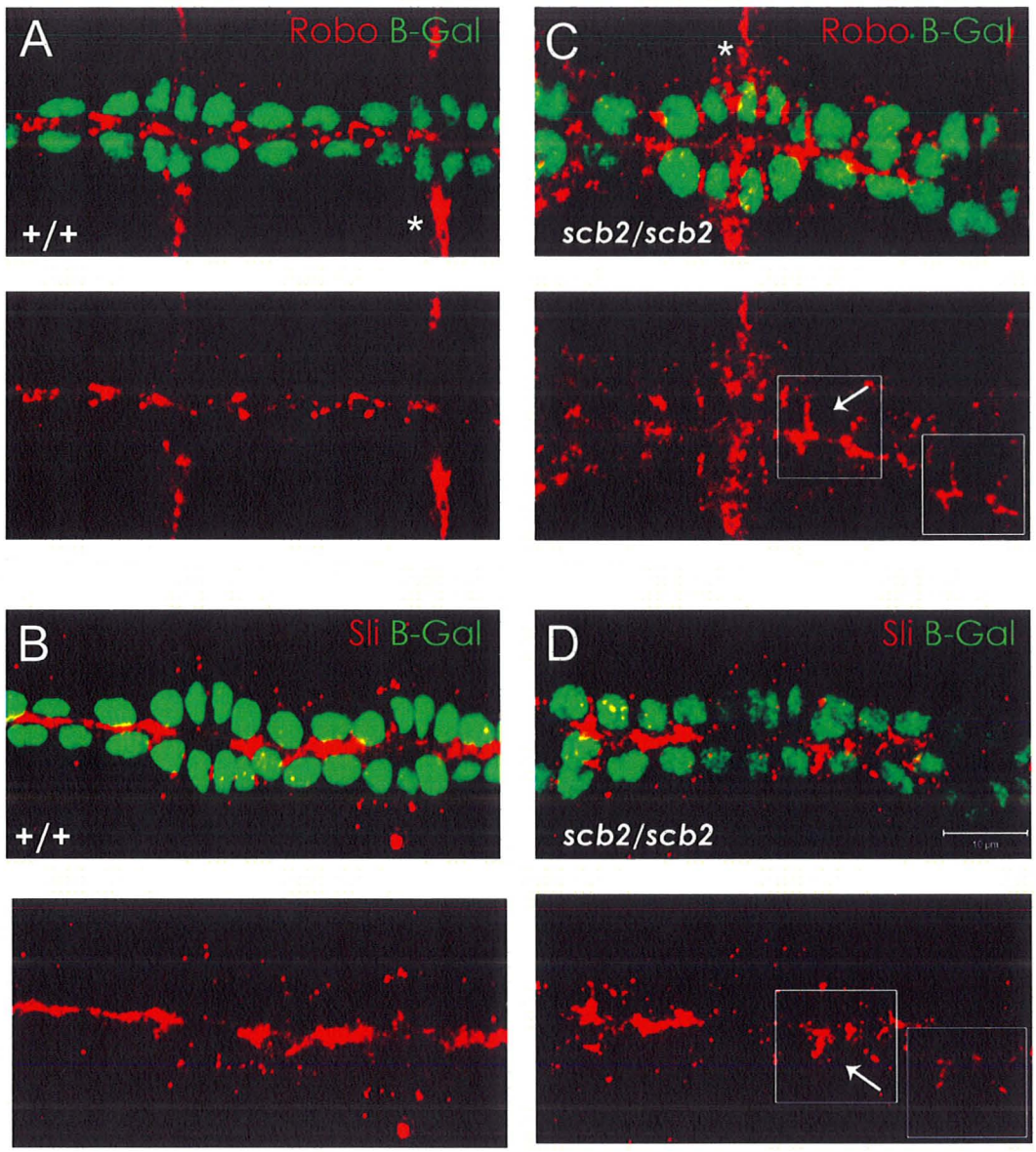
A
Robo B-Gal
+/+
*
C
*
Robo B-Gal
scb2/scb2
B
Sli B-Gal
+/+
D
Sli B-Gal
scb2/scb2

3.5 Overall cell polarity of cardioblasts is not disrupted in the absence of αPS3

Prior to merging at the midline, cardioblasts undergo a mesenchyme-to-epithelium transition and acquire apical-basal polarity (Frémion et al., 1999). Monoclonal antibody staining shows that Slit's localization is polarized at the apical surface of the cardioblasts (Fig. 2B). Robo is also polarized at the cardioblasts apical surfaces (Fig. 2A). In *slit* mutant embryos, the rows of cardial cells do not assemble properly and exhibit abnormal localization of several cell polarity markers (Qian et al., 2005; E. Santiago-Martinez et al., 2006) In the absence of αPS3 Slit and Robo fail to localize properly to the apical surface of cardioblasts. Therefore the question emerges: is cell polarity otherwise affected in *scab* mutants? To explore this, I examined cell polarity in the heart at stage 17 after cardioblast migration and lumen formation have occurred. I have looked at the distribution of three polarity markers in the heart. Discs-large (Dlg), a membrane-associated guanylate kinase protein (Woods, Hough, Peel, Callaini, & Bryant, 1996), that normally localizes to the apical-lateral surface of cardial cells in stage 16 embryos does not appear altered in *scab* mutants (Fig. 3.4A and D). Pericardin (Prc), a type IV collagen α-chain (Chartier et al., 2002) becomes concentrated at the basal surface of the cardioblasts and around the pericardial cells and is normally absent from the lumen of the heart (Fig. 3.4B). In *scab* mutants Pericardin expression in the heart is not significantly disrupted (Fig.3.4E). α-Spectrin, a membrane-bound cytoskeletal protein (Lee, Coyne,

Dubreuil, Goldstein, & Branton, 1993) that preferentially localizes to the basal-lateral surface of cardial cells (E. Santiago-Martinez et al., 2006) is also normal in *scab* mutant embryos which indicates that the CBs are correctly polarized (Fig. 3.4C and F). Together these data suggest that αPS3 is not required for heart cell polarity but instead functions at a later stage, once initial cell polarity has been established.

The localization of the cell junctional marker Par6 was also explored in the *Drosophila* heart. A GFP-tagged Par6 fusion protein was over-expressed in wild type and *scb2* backgrounds using the muscle specific driver *dMef-GAL4*. Over-expression under normal conditions (21-23°C) proved too powerful so embryos were incubated at 18°C to procure lower levels of expression. In polarized epithelia Par 6 localizes to the apical-lateral surface of cells. In this system, the over-expressed protein failed to provide any polarization information as its expression was strong throughout the entire surface of the cardial cells (Appendix 2 Fig.A2.4)

Figure 3.4: Cell polarity markers in wild type and *scab* mutant embryos.

If Slit fails to localize to the lumen in *scb2* mutant embryos, is cell polarity otherwise affected? To determine this we have looked at the distribution of three polarity markers in the heart. Discs-Large is typically distributed to the apical-lateral surface of cardioblasts [A]. α-Spectrin preferentially localizes to the basal-lateral surface of the heart cells [B]. Pericardin becomes concentrated at the basal surface of the cardial cells while signal in the lumen is minimal [C]. These cell polarity markers and are not significantly mislocalized in the absence of the alpha integrin [D-F] suggesting that cell polarization does not require the aPS3 integrin. Dorsal view of stage 16-17 wild type [A-C] and *scb2* mutant [D-F] embryos immunolabelled using anti-β-galactosidase to detect the B2-3-20 cardial cell enhancer trap (green) and MAb to detect polarity markers (red). Imaging was done using confocal microscopy. Anterior to the left. Calibration: 10μm

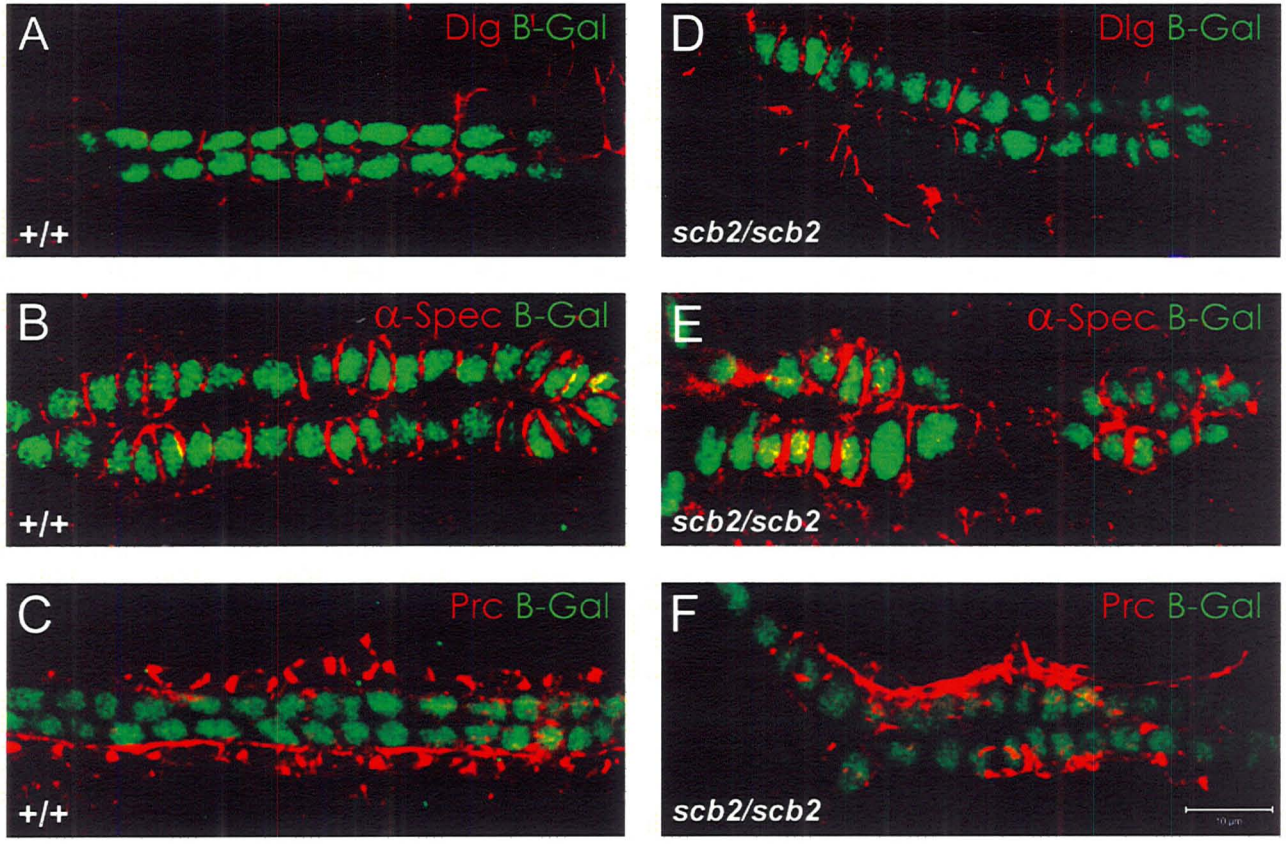
A
Dlg B-Gal
+/+
B
α-Spec B-Gal
+/+
C
Prc B-Gal
+/+
D
Dlg B-Gal
scb2/scb2
E
α-Spec B-Gal
scb2/scb2
F
Prc B-Gal
scb2/scb2

3.6 Over-expression of αPS3 partially restores Robo and Slit localization to the apical membrane of *scab* cardioblasts

Over-expression of αPS3 in a wild type background results in mild delays in heart closure (Fig 3.1D). When rescue experiments were performed using the *scab* transgene and the muscle specific driver *dMef-GAL4*, αPS3 was unable to restore the heart assembly phenotype (Table 3.1 and Fig.3.1E). However its over-expression is able to restore cell migration (Table 3.1 and Fig.3.1F). There is a secondary effect on heart morphology caused by a defect in dorsal closure. This secondary effect caused an array of phenotypes (Fig.3.1E and F) and resulted in an apparent insignificant diminution of *scb2* severity (Table 3.1). In addition, *scb2;UAS-scab/dMef-GAL4* embryos show no rescue of embryonic lethality (Appendix 2 Table A2.2). Interestingly, Robo and Slit localization was partially restored to the apical membrane of the cardioblasts even though the heart assembly phenotype was not (Fig.3.5E and F).

3.7 Requirement for Robo in Integrin localization

I performed immunohistochemical analysis to show αPS3 localization indirectly by staining for its dimerization partner βPS1 (*mys*). In wild type, βPS1 is localized to the apical and basal domains of the cardial cells as well as muscle insertions (Fig.3.6A). Surprisingly βPS1 was not mislocalized in *scab* mutants where it too localized to the apical and basal membrane of the cell (Fig.3.6B).

In embryos missing both Roundabout receptors expressed in the heart Robo (*robo*) and Robo2 (*lea*) βPS1 fails to localize to the apical and basal surfaces of the cardial cells and persists around the entire cell (Fig.3.6C) suggesting that integrin polarization may depend on Robo.

3.8 RNA interference mediated knockdown of αPS3 and βPS1

In order to further test the hypothesis that integrins are required for proper Slit and Robo apicalization and concentration to the heart lumen, a study using RNA interference (RNAi) was carried out. Knockdown was restricted to the muscle and heart cells by using the *dMef-GAL4* driver and for lethality analyses the ubiquitous driver *daughterless-GAL4* was used. *UAS-scabRNAi/ dMef-GAL4,B2-3-20* and *UAS-mysRNAi/ dMef-GAL4,B2-30 or UAS-scabRNAi/ da-GAL4 and UAS-mysRNAi/ da-GAL4* embryos were kept at 29°C to ensure a maximal over-expression of the dsRNA constructs.

Using the B2-3-20 cardial enhancer trap the effects on heart assembly of the RNAi mediated knockdown of αPS3 and βPS1 was assessed. Results revealed a mild effect on heart assembly, however some migration defects were observed although at a low frequency (Table 3.1 and Appendix 2 Fig. A2.3). Immunolabelling experiments, however, reveal an incomplete apicalization of both Slit and Robo in *UAS-scabRNAi/dMef-GAL4, B2-3-20* and *UAS-mysRNAi/dMef-GAL4, B2-3-20* embryos (Fig. 3.7C-F) suggesting that cardioblast cells require integrins to properly localize Slit and Robo in a cell-autonomous manner.

To confirm the effectiveness of the dsRNA constructs, lethality and adult viability assays were performed as well as molecular analysis (Appendix 2 Tables A2.3 and A2.4). Zygotic αPS3 and βPS1 expression is required to carry the *Drosophila* embryo through embryogenesis (Leptin et al., 1989; Stark et al., 1997), thus mutations in these genes exhibit embryonic lethality. Therefore, if protein knockdown mediated by dsRNA is effective, embryos over-expressing the dsRNA with a ubiquitous driver should not survive. After a 24-36 hour incubation at 29°C, *UAS-scabRNAi;da-GAL4* and *UAS-mysRNAi;da-GAL4* hatched versus unhatched (fertilized and unfertilized) embryos were counted and percent lethality was calculated as outlined in the Materials and Methods. This assay revealed a low rate of lethality (*UAS-scbRNAi;da-GAL4* 5% lethality and *UAS-mysRNAi;da-GAL4* 10% lethality, Appendix 2 Table A2.4). The experiment was performed with the muscle specific driver *dMef-GAL4* as well (Appendix 2 Table A2.4). Adult viability where the numbers of eclosed adults was counted revealed a pupal lethality when *UAS-scbRNAi* was expressed ubiquitously and a young larval lethality when *UAS-mysRNAi* was expressed (Appendix 2 Table A2.4). Together these data suggest that the protein knockdown for both αPS3 and βPS1 may not be complete.

To explore this further, immunoblotting was performed on extracts from *UAS-scabRNAi/da-GAL4* embryonic tissue. Western blots containing 150μg of protein per lane were incubated with the rabbit polyclonal antiserum generated against the N-terminus of the αPS3 integrin. This antiserum recognizes the over-

expressed full-length protein (~125kDa) but not the endogenous protein (Appendix 2 Fig. A2.3). Without a baseline signal obtained from endogenous expression of αPS3 it is not possible to make the knockdown assessment.

βPS1 knockdown was explored through immunolabelling due to a lack of antisera suitable for immunoblotting. *UAS-mysRNAi* and the *dMef-GAL4* driver were used to knockdown βPS1 protein production in the muscle and heart cells. Immunolabelling using a MAb for βPS1 and antiserum raised against dMEF2 was done on *UAS-scabRNAi/dMef-GAL4* embryos. Staining revealed a lack of knockdown of the protein as signal was still detectable at very strong levels throughout the musculature of the embryo (Appendix 2 Fig.A2.3).

Figure 3.5: Expression of αPS3 partially restores Slit and Robo localization

In wild type embryos Robo [A] and Slit [B] accumulate apically in the lumen while *scb2* mutant embryos reveal lateral accumulation of Robo and Slit between the cardioblasts (arrows) [C-D]. αPS3 was expressed in *scb2* embryos by the muscle specific driver dMef-GAL4. Robo and Slit localization to the apical domain of the cells was partially restored [E-F]. Residual Robo and Slit lateral accumulation can be observed (arrows). Embryos were immunolabelled using anti-β-galactosidase to detect the B2-3-20 cardial cell enhancer trap (green) and MAb to detect Slit and Robo (red) imaged using confocal microscopy. All images are dorsal views. Anterior to the left. Calibration: 10μm

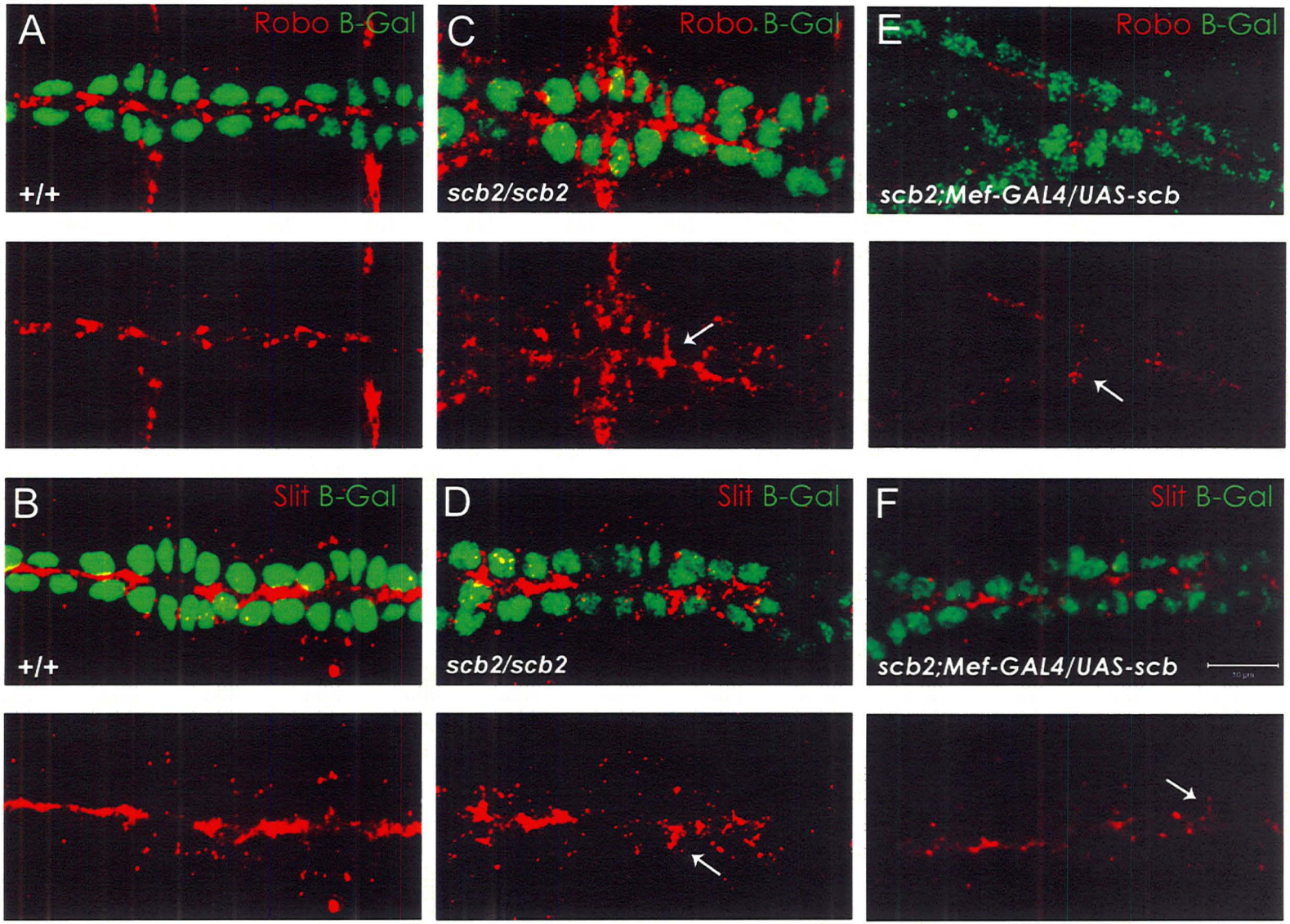
A
Robo B-Gal
+/+
C
Robo B-Gal
scb2/scb2
E
Robo B-Gal
scb2;Mef-GAL4/UAS-scb
B
Slit B-Gal
+/+
D
Slit B-Gal
scb2/scb2
F
Slit B-Gal
scb2;Mef-GAL4/UAS-scb

Figure 3.6: Integrins are mislocalized in the absence of Robo

In order to examine integrin behaviour in the heart stage 16-17 embryos were labelled using antibodies against the βPS1 integrin (red) and for the muscle marker Mef2 (green). In wild type embryos βPS1 decorates the apical and basal membranes of the cardioblasts as well as muscle attachments [A]. Interestingly, in *scb2* embryos βPS1 is not mislocalized, maintaining its basal-apical polarity and muscle attachment integrity [B] although its levels are reduced. In embryos missing both Roundabout receptors expressed in the heart Robo (*robo*) and Robo2 (*lea*) βPS1 is no longer polarized in the cardial cells but remains over the entire surface (inset) [C]. Muscle attachment localization is also diffuse (asterisk). All images are dorsal views. Anterior to the left.

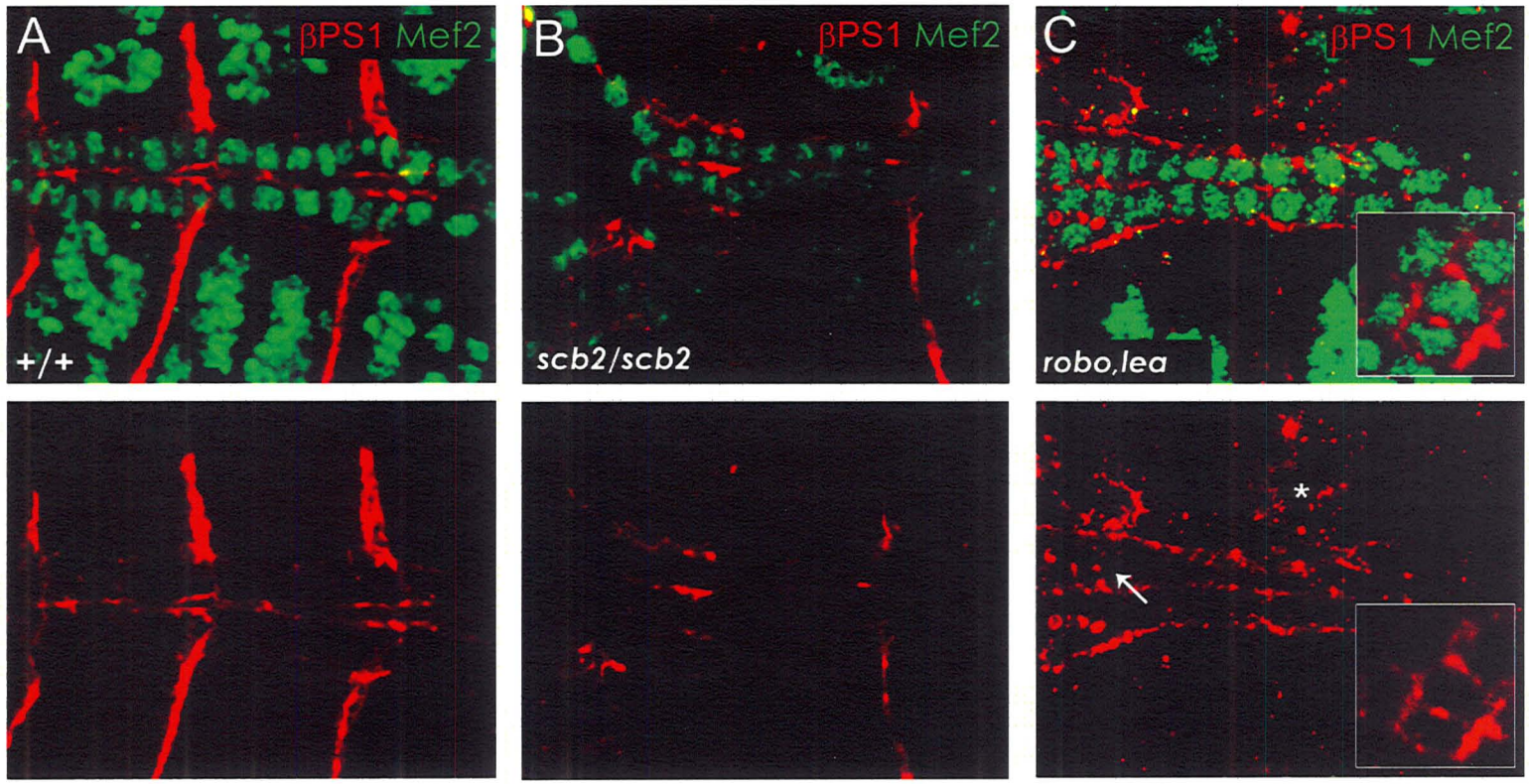
A
βPS1 Mef2
+/+
B
βPS1 Mef2
scb2/scb2
C
βPS1 Mef2
robo,lea
*

Figure 3.7: Apicalization of Slit and Robo requires Integrins cell autonomously.

In wild type embryos Slit and Robo accumulate apically in the lumen [A-B]. In *scb2* embryos there are reduced levels of Slit and Robo as compared to the wild type controls and furthermore, Slit and Robo persist on lateral cells surfaces. dsRNA for each subunit of the integrin dimer was expressed using the muscle specific driver dMef-GAL4,. *scab* (αPS3) [C-D] and *myospheroid* (βPS1) [E-F] knockdowns display a marked delay in apicalization seen as lateral signal (arrows). Together these data suggest that integrins function in Slit and Robo localization in a cell autonomous manner. All embryos were immunolabelled using anti-β-galactosidase to detect the B2-3-20 cardial cell enhancer trap (green) and MAb to detect Slit and Robo (red) and imaged using confocal microscopy. All images are dorsal views. Anterior to the left. Calibration: 10μm

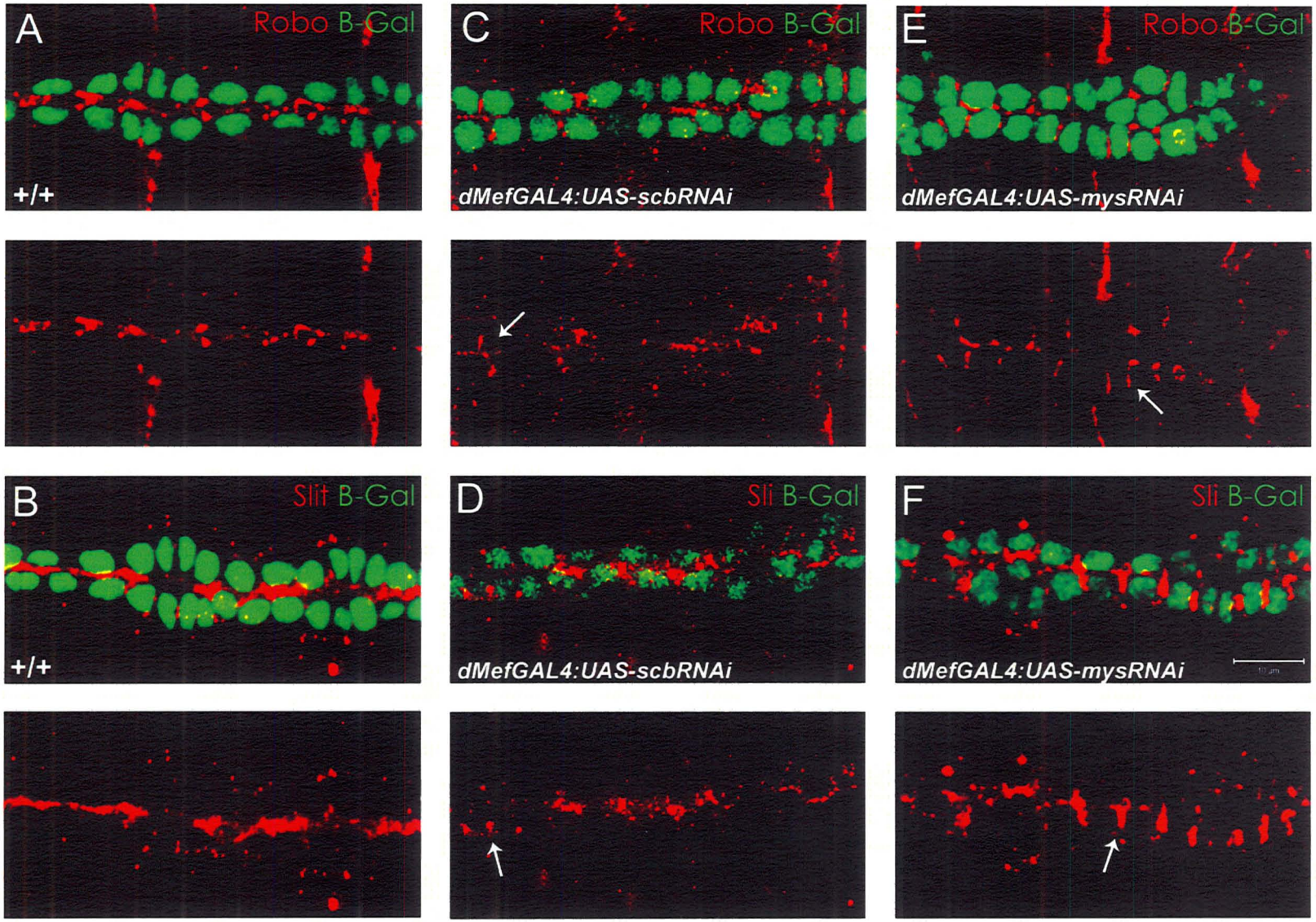
A
Robo B-Gal
+/+
C
Robo B-Gal
dMefGAL4:UAS-scbRNAi
E
Robo B-Gal
dMefGAL4:UAS-mysRNAi
B
Slit B-Gal
+/+
D
Sli B-Gal
dMefGAL4:UAS-scbRNAi
F
Sli B-Gal
dMefGAL4:UAS-mysRNAi

Table 3.1 Frequency of heart assembly defects in αPS3 mutants

Genotype	*yw*	*scb*^{2}	*scb*^{01288}	*scb*^{2};*UAS-scb/DmefGAL4*	*scb*^{2};*UAS-scbΔC/DmefGAL4*	*UAS-scb/DmefGAL4*	*UAS-scbΔC/DmefGAL4*
Severity	0.5	2.5	2.7	2.2	2.8	1.1	2.8
Penetrance	0.15	0.85	1.00	0.79	0.90	0.14	0.90
Irreg. Migration	0	16	11	8	18	0	9
Cell Clumps	0	21	22	23	29	3	22
Midline Crossing	5	3	13	3	0	3	16
Other[a]	8	25	47	21	22	18	41
Total Embryos	20	20	20	20	20	20	20

a Other includes: twists, gaps and delayed migration (including dorsal closure).

Table 3.2 Frequency of heart assembly defects in RNA interference experiments

Genotype	*yw*	*UAS-scbRNAi/DmefGAL4*	*UAS-mysRNAi/DmefGAL4*
Severity	0.5	1.9	1.00
Penetrance	0.15	0.63	0.40
Irreg. Migration	0	14	3
Cell Clumps	0	12	0
Midline Crossing	5	12	2
Other[a]	8	18	17
Total Embryos	20	20	20

a Other includes: twists, gaps and delayed migration (including dorsal closure).

Chapter four: DISCUSSION

The *Drosophila* heart arises from the dorsal migration and subsequent fusion of bilateral rows of cardioblasts into a single tube at the midline. Previous studies have shown that the coordinated migration and formation of a lumen in the *Drosophila* heart requires signaling by Slit which is secreted by the cardioblasts and binds to Robo receptors on the same cells (MacMullin & Jacobs, 2006; E. Santiago-Martinez et al., 2008). The cardioblasts of embryos lacking Slit function fail to align properly at the dorsal midline as a result of slower and incomplete migration and fail to form a lumen.

Cardioblasts also express a single Integrin dimer, αPS3/βPS1 (Stark et al., 1997). Integrins are a family of transmembrane receptors and key factors in cell migration and cell matrix adhesion. Previous work has shown that Slit interacts genetically with mutations in both the α and β subunits of the PS integrins in a dosage sensitive manner within the nervous system (Stevens & Jacobs, 2002) and the heart (MacMullin & Jacobs, 2006). Like Slit, Integrins are similarly required for proper assembly of the heart. When gene dosage in the Slit and Integrin pathways are altered simultaneously, there are more than additive effects on phenotype, suggesting that the two pathways converge upon a common function. To this date there are no known analyses of Integrin function in heart morphogenesis.

The purpose of this thesis was to explore the function of αPS3 (*scab*) in heart morphogenesis in the context of Slit and Robo signalling. The work outlined in this thesis shows a requirement for the αPS3 integrin in *Drosophila* heart morphogenesis and lumen formation. The lack of accumulation of Slit and Robo in the lumen of the heart, and unusual sub-apical localization after RNAi induced knockdown suggests a role for the integrins in regulating heart cell polarization. However, other markers of cell polarization are not significantly disrupted in αPS3 null embryos. In addition, in the absence of Robo, integrins fail to localize to the apical and basal surface of the cardioblasts. Therefore Integrin and Slit/Robo are functionally interdependent, and likely co-operate in heart morphogenesis.

4.1 Specificity of the αPS3 polyclonal antibody

The generation of an antibody that specifically recognizes αPS3 was necessary in order to explore integrin behavior in the heart. The antiserum generated recognized the over-expression of the transgenic protein as well as an unidentified band migrating just above the 150kDa mark. When tested through immunohistochemistry, the antibody failed to give a specific signal for endogenous αPS3 but recognizes the over-expressed integrin. These data suggest that the antibody is specific for the transgenic but not the endogenous protein. This may be unlikely as the DNA extracted from a yw-;+;+ fly that was amplified using the same primers designed to clone the antigenic fragment and sequenced shows 100% identity to the pUAST-scab sequence and to the amplified DNA used to create the antigenic protein fragment. Interestingly, it was

found that there are 18 extra base pairs in the sequence reported in FlyBase causing a 6 amino acid gap during the alignment (Appendix 2 Fig. A2.5).

There is the possibility that the observed >150kDa band is in fact αPS3. Proteins can undergo posttranslational modifications that may shift their predicted molecular weight. If this were the case of αPS3 it could migrate at a higher molecular weight depending on the number and type of posttranslational modification. Sequencing the protein in question is the most direct way of confirming this; however it can be difficult and costly. Co-immunoprecipitation assays are an indirect but perhaps an easier way to address whether or not the antibody is specific to αPS3 by blotting for known co-factors that associate with the integrin.

4.2 Integrins are required for heart and lumen formation

The αPS3/βPS1 is the only known integrin dimer in the heart (Stark et al., 1997). Severe defects in heart morphogenesis were seen in embryos lacking αPS3 (*scb*). Errors included irregular migration of cardial cells towards the dorsal midline, delayed closure of the heart and cell clumping (Fig.3.1B-C). Electron microscope transverse sections of the dorsal vessel of αPS3 deficient embryos revealed a requirement for the αPS3/βPS1 integrin in lumen formation (Fig 3.2).

4.21 Effects of Dorsal Closure in heart analyses

Dorsal closure is the migration of the ectoderm towards the dorsal side of the embryo that results in the enclosure of the gut and the amnioserosa. The αPS3/βPS1 integrin is expressed in the amnioserosa and mutations in both αPS3 and βPS1 result in dorsal closure defects. Migrating cardial cells maintain close contact with the leading edge of the migrating ectoderm, so that heart formation cannot proceed unless dorsal closure is complete (Rugendorff et al., 1994). In embryos homozygous for a null allele of scab (*scb2*) the severe heart disruption observed was most likely due to an incomplete dorsal closure. This effect makes the assessment of the phenotype difficult as only the cells located at the posterior of the dorsal vessel come into contact at the midline. Because of this, analysis of dorsal vessel morphogenesis was done in the posterior chamber of the heart. The hypomorphic allele *scb01288* has less severe dorsal closure-related effects allowing for the cardial cells to migrate further towards the midline allowing for primary defects in heart assembly to become more obvious. This explains the discrepancy observed in the calculated severity for both alleles (compare 2.5 (*scb2*) vs. 2.7 (*scb01288*) Table 3.1). In retrospect, an allele displaying more defects that are not secondary in nature to dorsal closure would have better suited for rescue analyses.

For the correct assessment of αPS3 function in heart morphogenesis it is important to uncouple the effects of dorsal closure since alteration in heart morphogenesis may be due indirectly to defects in the dorsal ectoderm. There

have been reports where it was possible to uncouple dorsal closure from cardial migration. Embryos of mutant allele of the *puckered* (*puc*) gene (involved in the JNK pathway during dorsal closure) proceed to a complete dorsal closure even though the two rows of cardial epithelial cells and the attached pericardial cells did not join at the dorsal midline (Chartier et al., 2002). In addition, analysis in embryos doubly heterozygous for *slit* and *scab* showed that the heart defects observed are independent of dorsal closure (MacMullin & Jacobs, 2006) (Appendix 1 Fig. 1A.6). However, this has not been the case when focusing solely on integrins. One way to address this would be to over-express αPS3 in the cells of the amnioserosa in hopes to rescue the dorsal closure phenotype. In this context, the effects of αPS3 on heart cell migration could be properly assessed. In *scb01288* embryos, heart cell migration can be observed medial to the ectodermal dorsal hole (Figure 3.1C); however this could be due to a detachment and subsequent retraction of the overlying ectoderm. This could be explored by immunolabelling the cardial cells using the α-dMef2 antibody which decorates the nuclei of muscle and heart cells and with α-phosphoTyrosine which outlines the cellular membrane of all cells. This method has been previously used to assay dorsal closure (MacMullin & Jacobs, 2006). The cells of the ectodermal leading edge and amnioserosa can be visualized simultaneously with cardial cell position in embryos (Appendix 1 Fig.A1.6). In wild type, during early dorsal closure, cardial cells are seen 1 to 2 cell lengths away from the amnioserosa and the leading edge is easily visualized. At late dorsal closure the cardial cells are

seen to align with the edge of the amnioserosa. Dorsal closure is incomplete in *scab* mutant embryos, with the cardial cells migrating much closer in proximity to the amnioserosa during early and late development (MacMullin & Jacobs, 2006). With this method the effect of dorsal closure on heart cell migration in *scb01288* embryos could be visualized, if the heart cells are migrating past the leading edge after dorsal closure arrest or the dorsal hole observed is simply an effect of a detached ectoderm.

4.3 Integrins may have a role in cardioblast cell migration

When embryos lack integrin function, the developmental processes that require integrins are revealed in the form of defects. For example, involution of the mesoderm does not require integrin function, since removal of the βPS1 subunit did not lead to gastrulation defects (Leptin et al., 1989). However, the primordial midgut cells require integrins since removal of αPS2/βPS1 or αPS1/βPS1 results in defective midgut migration (M. D. Martin-Bermudo et al., 1999). In *scab* mutant embryos we observe irregular migration of cardial cells towards the midline, suggesting that the migration of these cells depends, at least in part, on integrin function. Stark et al. reported more severe dorsal vessel defects when βPS1 is absent than when αPS3 is missing (Stark et al., 1997), suggesting that the αPS3/βPS1 integrin may not be the only integrin functioning in the heart. It would be interesting to analyze heart assembly in integrin double mutants to explore this hypothesis.

The over-expression of αPS3 in a wild type background does not have a significant effect in heart assembly although cell migration appears mildly delayed (Fig. 3.1D). Rescue experiments over-expressing αPS3 in *scb2* mutants showed restoration of cell migration as the two rows of cardioblasts appear to have re-gained their continuity (Fig.3.1E-F). Other defects such as delayed heart closure showed no amelioration, however this may result from the inability to rescue dorsal closure since expression was directed to the muscle only. Nevertheless, these observations suggest that αPS3 may be involved in cardial cell migration early in dorsal vessel development.

4.4 Integrins may have an adhesive function in the heart

It has been shown in the *Drosophila* embryo, that normal morphogenesis requires the *α* subunit cytoplasmic domain to control integrin adhesion. Over-expression of a cytoplasmically truncated αPS2/βPS1 integrin resulted in an excessively active receptor as muscles containing the mutant integrin made extra muscle attachments at aberrant positions on the muscle surface (M. D. Martin-Bermudo et al., 1998a). This suggests that the α subunit cytoplasmic tail of the integrin dimer is required for the inside-out regulation of integrin affinity. Similar observations have been made with vertebrate integrins (cited by (M. D. Martin-Bermudo et al., 1998b)). The over-expression of an αPS3 transgene with enhanced adhesive properties caused a dominant phenotype in heart assembly when expressed in a wild type background and was not able to restore overall heart morphology of the mutant (Table 3.1). However, apparent inability to

restore morphology could be an artifact introduced by the scoring method, since even though there appears to be more instances of irregular migration, the overall morphology of the heart is restored compared to that of the null (Fig3.1I). The dominant effects observed upon αPS3ΔC over-expression, however, are suggestive of an increased adhesiveness conferred upon the cardioblast cells.

Previous genetic data suggest that Slit signalling is dependent on adhesive signals from the αPS3/βPS1 integrin (MacMullin & Jacobs, 2006) (see Appendix 1). In *scb2* mutants Slit and Robo function in lumen formation seems impaired perhaps by a lack of apicalization and/or concentration in the luminal surface (See section 4.5). When αPS3ΔC is expressed in these mutants, lumen formation is partially restored suggesting that *slit* and *robo* function may be partially dependent on αPS3 adhesive properties to establish a lumen. It would be interesting to explore Slit and Robo localization when the αPS3ΔC transgene is expressed in a wild type background and if it would be sufficient to rescue Slit and Robo localization in mutants.

4.5 Integrins may be required for Slit and Robo localization and/or stabilization to the apical membrane of cardioblasts and are downstream of polarizing signals

Robo and Slit are first detected surrounding the cell membrane at stage 13-14 of embryogenesis. Upon midline convergence of the cardioblasts, Slit and Robo become polarized at the cell's apical surface (Fig 3.3A-B). In *scb2* embryos, Slit and Robo apicalization is incomplete (Fig.3.3C-D) and this delay in

apicalization can be partially restored by over-expressing αPS3 in the muscle and cardial cells (Fig. 3.5) suggesting that there is a requirement for Integrin function in Robo and Slit apicalization. This is supported by the muscle-specific dsRNA mediated knockdown of αPS3 and βPS1 that resulted in incomplete apicalization of Slit and Robo (Fig. 3.7).

Immunolabelling studies in *scab* mutant embryos reveal a reduction of Robo and Slit signal as compared to their wild type counterparts (Fig. 3.3 insets at same gain as control) suggesting that integrins may also work to stabilize Slit and/or concentrate Robo at the apical membrane. Of concern while analyzing this data is the observation that embryos homozygous for *scb2* seem to stain less intensely than the wild type ones. Within the same embryo population there is great variance in the levels of immunofluorescence. Therefore it may be necessary to address this aspect of integrin function in another more quantitative way. If integrins are acting to stabilize Robo at the apical surface but not to localize it, increasing Robo expression in a *scab* mutant background should restore apicalization of Slit and Robo. However if integrins are responsible for Robo localization, over-expression of Robo should not alter the incomplete apicalization observed.

Apicalization of both Slit and Robo is necessary for establishing a luminal surface in heart cells. In wild type embryos, Discs-Large (Dlg) and α-Spectrin are located basal-laterally in the migrating cardioblasts. Once they reach the midline and contact their contralateral partners the switch to an apical-lateral polarity. In

slit and *robo* mutants, Dlg and α-Spectrin localization is disrupted, however the polarity phenotype is observed only upon heart assembly suggesting that Slit and Robo are not required for initiating polarity but rather for correctly switching it (Qian et al., 2005). Since Slit and Robo are not fully apical in the absence of integrins cell polarity was examined. Results show that polarization of the cardioblast cells in the absence of integrins is not significantly disrupted. This suggests that Integrins function downstream of polarity signals. It could be that the polarization of the markers used is not dependent upon integrin function and perhaps other markers of cell polarity would be more useful. The expression of the junctional marker Par6 was explored (Fig A2.4) however, this too yielded little information on heart polarity as the over-expressed GFP fusion protein did not seem to preferentially localize. An interesting route to explore might be DE-cadherin as the most current heart lumen formation model suggests that Slit and Robo act to localize DE-cadherin to the sites of contact between the cardioblasts while creating an area of "repulsion" in the lumen (Fig 1.2C) (E. Santiago-Martinez et al., 2008). In *scb2* mutants, cardioblasts seem to have extensive apical adhesion (Fig 3.2). Perhaps in the absence of integrins, Slit and Robo are no longer able to displace DE-cadherin and it would be localized to the entirety of the apical membrane thus providing a useful marker of cell polarity.

4.6 Integrins may be downstream of Robo's polarizing signal

In wild type βPS1 is localized to the apical and basal surfaces of the cardial cells (Fig.3.6A) Integrins are obligate heterodimeric proteins. They must first assemble into a heterodimer to form a functional receptor that is transported to the cell surface (Leptin et al., 1989; M. D. Martin-Bermudo, Dunin-Borkowski, & Brown, 1997) The absence of αPS3 should have resulted in the mislocalization or loss of βPS1. However proper localization of βPS1 upon heart closure in *scb2* mutants (Fig3.6B), suggests that there might be compensation by the other integrin α subunits. In the midgut, loss of just one α subunit results in either a modest delay (αPS1) or no effect (αPS3) in migration, thus there is partial redundancy in the function of αPS1/βPS1 and αPS3/βPS1 integrins (M. D. Martin-Bermudo et al., 1999). It should be noted that both integrin dimers are expressed in the gut and this is not the case for the heart.

If integrins are not mislocalized in the absence of αPS3 could Robo and Slit be directing its localization? Indeed, in the absence of Robo, integrins were found over the entire surface of the cell (Fig 3.6C) rather than at the basal-apical membranes. To ascertain the requirement for Robo in integrin polarization, it is necessary to investigate whether expression of Robo in a *robo* mutant background is able to restore Integrin localization. Similar experiments should be conducted with Slit to determine whether this is a process involving Slit/Robo signalling.

4.7 Cell autonomy

Although the αPS3/βPS1 integrin dimer is the only one expressed in the heart, indirect effects of eliminating αPS3 cannot be ruled out because of its function in other tissues, such as the amnioserosa involved in dorsal closure. By performing tissue- and cell-type-specific rescue experiments one can address the cell autonomy of these requirements and rule out secondary effects. αPS3 expression within the muscle cells is sufficient to partially restore the localization of Slit and Robo to the apical membrane of the heart but not morphology. Conversely, RNA interference of αPS3 or βPS1 protein expression in the muscle and heart cells shows the same apicalization defects observed with mutations for αPS3 but fail to show cause severe cell migration or heart assembly defects (Table 3.2 and Appendix 2 Fig A2.3). Together these data suggest that integrins function to localize Slit and Robo in a cell autonomous manner.

Whether these dsRNA constructs are able to properly knockdown αPS3 and βPS1 was explored, however the methods implemented proved inefficient. .Maternal contribution of αPS3 or βPS1 was not removed in these experiments. Only a small amount of αPS3 RNA is present in 0-2 hour embryos (Stark et al., 1997) but, this small contribution of maternal RNA might be enough to mask the effects of RNAi mediated knockdowns.

4.8 Concluding Remarks and Future Directions

The work outlined has demonstrated a role for Robo in directing proper integrin localization to the basal-apical membranes of the cardial cells and conversely, a requirement for integrins in proper apicalization of Slit and Robo. This suggests that the relationship between Slit/Robo and Integrin signalling is not a simple one although it seems clear that Slit/Robo signalling depends upon Integrin adhesive properties. However this research suggests that Integrins and Robo act together to establish cell polarity in cardioblast cells. How is this achieved remains a question to be further explored.

Integrins could contribute to heart formation by mediating adhesion to the extracellular matrix so that cells are kept close to the source of signals (Slit and Robo). Alternatively, ECM signals could be transmitted by integrin signalling pathways where integrins may be involved in actively transmitting signals from the ECM by an integrin-specific signalling cascade or as integrins recruit a large number of effector proteins (Zaidel-Bar, Itzkovitz, Ma'ayan, Iyengar, & Geiger, 2007), it could be that they are required to organize intracellular signalling centers to relay signals from the ECM to the interior of the cell. Another alternative is that integrin-mediated adhesion to the ECM could be essential for other types of cell surface receptors to bind ECM ligands and transduce signals. Syndecans can act as co-receptors with integrins and research in the Jacobs lab has suggested a requirement for *Drosophila* Syndecan (*sdc*) in heart morphogenesis. In the absence of Syndecan, like with Integrins, Slit is no longer localized to the apical

membrane of the heart cells, but it is found over the entire surface of the cells. Since biochemical data already suggests a ternary complex between Slit, Robo and Syndecan, it could be that this complex in the heart needs Integrin function as well. To address this it would be useful to explore the localization of Slit and Robo in embryos doubly heterozygous for *sdc* and *scb* where both are partially reduced. If the ternary complex acts to stabilize and concentrate Slit at the lumen it could be that the phenotype observed would be similar to the one seen for both mutants.

In addition, research shows that there is crosstalk between integrins and TGF-β signalling. TGF-β stimulates integrin expression by controlling the transcription of genes that encode numerous integrins in several cell types and tissues, as well as in various human cancers (Margadant & Sonnenberg, 2010). Interestingly, Integrins seem to be involved in the activating and signalling through the TGF-β receptor as well, suggesting there might be a feedforward loop in regulating both receptors (Margadant & Sonnenberg, 2010). Studies in cancer and wound healing reveal roles for both receptors in the deposition of extracellular matrix needed for migrating cells and modulating the migrating behaviour itself (Margadant & Sonnenberg, 2010). Although more research would have to be done to provide evidence for this, it could be that Integrins and Robo have a similar relationship where there is no clear hierarchy established between both signalling pathways but they rather act in a feedforward loop promoting each other's function.

BIBLIOGRAPHY

Andrew, D. J., & Ewald, A. J. (2010). Morphogenesis of epithelial tubes: Insights into tube formation, elongation, and elaboration. *Developmental Biology, 341*(1), 34-55. doi:10.1016/j.ydbio.2009.09.024

Autiero, M., De Smet, F., Claes, F., & Carmeliet, P. (2005). Role of neural guidance signals in blood vessel navigation. *Cardiovascular Research, 65*(3), 629-638. doi:10.1016/j.cardiores.2004.09.013

Bass, M. D., Morgan, M. R., & Humphries, M. J. (2009). Syndecans shed their reputation as inert molecules. *Science Signaling, 2*(64), pe18. doi:10.1126/scisignal.264pe18

Battye, R., Stevens, A., & Jacobs, J. R. (1999). Axon repulsion from the midline of the drosophila CNS requires slit function. *Development (Cambridge, England), 126*(11), 2475-2481.

Bier, E., Vaessin, H., Shepherd, S., Lee, K., McCall, K., Barbel, S., Ackerman, L., Carretto, R., Uemura, T., & Grell, E. (1989). Searching for pattern and mutation in the drosophila genome with a P-lacZ vector. *Genes & Development, 3*(9), 1273-1287. Retrieved from http://genesdev.cshlp.org/content/3/9/1273.abstract

Bodmer, R., & Venkatesh, T. V. (1998). Heart development in drosophila and vertebrates: Conservation of molecular mechanisms. *Developmental Genetics, 22*(3), 181-186. doi:2-2

Bogaert, T., Brown, N., & Wilcox, M. (1987). The drosophila PS2 antigen is an invertebrate integrin that, like the fibronectin receptor, becomes localized to muscle attachments. *Cell, 51*(6), 929-940.

Bokel, C., & Brown, N. H. (2002). Integrins in development: Moving on, responding to, and sticking to the extracellular matrix. *Developmental Cell, 3*(3), 311-321.

Bradford, M. M. (1976). A rapid and sensitive method for the quantitation of microgram quantities of protein utilizing the principle of protein-dye binding.. *Analytical Biochemistry, 72*, 248.

Brower, D. L., Bunch, T. A., Mukai, L., Adamson, T. E., Wehrli, M., Lam, S., Friedlander, E., Roote, C. E., & Zusman, S. (1995). Nonequivalent requirements for PS1 and PS2 integrin at cell attachments in drosophila: Genetic analysis of the alpha PS1 integrin subunit. *Development (Cambridge, England), 121*(5), 1311-1320.

Brown, N. H. (1994). Null mutations in the alpha PS2 and beta PS integrin subunit genes have distinct phenotypes. *Development (Cambridge, England), 120*(5), 1221-1231.

Brown, N. H., Gregory, S. L., & Martin-Bermudo, M. D. (2000). Integrins as mediators of morphogenesis in drosophila. *Developmental Biology, 223*(1), 1-16. doi:10.1006/dbio.2000.9711

Chanana, B., Steigemann, P., Jackle, H., & Vorbruggen, G. (2009). Reception of slit requires only the chondroitin-sulphate-modified extracellular domain of syndecan at the target cell surface. *Proceedings of the National Academy of Sciences of the United States of America, 106*(29), 11984-11988. doi:10.1073/pnas.0901148106

Chartier, A., Zaffran, S., Astier, M., Semeriva, M., & Gratecos, D. (2002). Pericardin, a drosophila type IV collagen-like protein is involved in the morphogenesis and maintenance of the heart epithelium during dorsal ectoderm closure. *Development (Cambridge, England), 129*(13), 3241-3253.

Chen, J. N., & Fishman, M. C. (2000). Genetics of heart development. *Trends in Genetics : TIG, 16*(9), 383-388.

Cripps, R. M., & Olson, E. N. (2002). Control of cardiac development by an evolutionarily conserved transcriptional network. *Developmental Biology, 246*(1), 14-28. doi:DOI: 10.1006/dbio.2002.0666

David, D. J. V., Tishkina, A., & Harris, T. J. C.The PAR complex regulates pulsed actomyosin contractions during amnioserosa apical constriction in drosophila. *Development, 137*(10), 1645-1655. doi:10.1242/dev.044107

Dejana, E., Bazzoni, G., & Lampugnani, M. G. (1999). Vascular endothelial (VE)-cadherin: Only an intercellular glue? *Experimental Cell Research, 252*(1), 13-19. doi:10.1006/excr.1999.4601

Devenport, D., & Brown, N. H. (2004). Morphogenesis in the absence of integrins: Mutation of both drosophila beta subunits prevents midgut migration. *Development (Cambridge, England), 131*(21), 5405-5415. doi:10.1242/dev.01427

Dickson, B. J., & Gilestro, G. F. (2006). Regulation of commissural axon pathfinding by slit and its robo receptors. *Annual Review of Cell and Developmental Biology, 22*, 651-675. doi:10.1146/annurev.cellbio.21.090704.151234

Drubin, D. G., & Nelson, W. J. (1996). Origins of cell polarity. *Cell, 84*(3), 335-344.

Frémion, F., Astier, M., Zaffran, S., Guillèn, A., Homburger, V., & Sémériva, M. (1999). The heterotrimeric protein go is required for the formation of heart epithelium in drosophila. *The Journal of Cell Biology, 145*(5), 1063-1076. doi:10.1083/jcb.145.5.1063

Gajewski, K., Choi, C. Y., Kim, Y., & Schulz, R. A. (2000). Genetically distinct cardial cells within the drosophila heart. *Genesis (New York, N.Y.: 2000), 28*(1), 36-43.

Grotewiel, M. S., Beck, C. D. O., Wu, K. H., Zhu, H. R., & Davis, R. L. (1998). Integrin-mediated short-term memory in *drosophila*. *Nature,* (391), 455-460.

Haag, T. A., Haag, N. P., Lekven, A. C., & Hartenstein, V. (1999). The role of cell adhesion molecules in drosophila heart morphogenesis: Faint sausage, shotgun/DE-cadherin, and laminin A are required for discrete stages in heart development. *Developmental Biology, 208*(1), 56-69. doi:10.1006/dbio.1998.9188

Hughes, P. E., Oertli, B., Han, J., & Ginsberg, M. H. (2001). R-ras regulation of integrin function. *Methods in Enzymology, 333*, 163-171.

Huminiecki, L., Gorn, M., Suchting, S., Poulsom, R., & Bicknell, R. (2002). Magic roundabout is a new member of the roundabout receptor family that is endothelial specific and expressed at sites of active angiogenesis. *Genomics, 79*(4), 547-552. doi:10.1006/geno.2002.6745

Hynes, R. O. (2004).
The emergence of integrins: A personal and historical perspective *Matrix Biology, 23*(6), 333-340.

Hynes, R. O. (2002). Integrins: Bidirectional, allosteric signaling machines. *Cell, 110*(6), 673-687.

Johnson, K. G., Ghose, A., Epstein, E., Lincecum, J., O'Connor, M. B., & Van Vactor, D. (2004). Axonal heparan sulfate proteoglycans regulate the distribution and efficiency of the repellent slit during midline axon guidance. *Current Biology, 14*(6), 499-504. doi:DOI: 10.1016/j.cub.2004.02.005

Kadam, S., McMahon, A., Tzou, P., & Stathopoulos, A. (2009). FGF ligands in drosophila have distinct activities required to support cell migration and differentiation. *Development (Cambridge, England), 136*(5), 739-747. doi:10.1242/dev.027904

Kidd, T., Bland, K. S., & Goodman, C. S. (1999). Slit is the midline repellent for the robo receptor in drosophila. *Cell, 96*(6), 785-794.

Kidd, T., Brose, K., Mitchell, K. J., Fetter, R. D., Tessier-Lavigne, M., Goodman, C. S., & Tear, G. (1998). Roundabout controls axon crossing of the CNS midline and defines a novel subfamily of evolutionarily conserved guidance receptors. *Cell, 92*(2), 205-215.

Klingseisen, A., Clark, I. B., Gryzik, T., & Muller, H. A. (2009). Differential and overlapping functions of two closely related drosophila FGF8-like growth factors in mesoderm development. *Development (Cambridge, England), 136*(14), 2393-2402. doi:10.1242/dev.035451

Kramer, S. G., Kidd, T., Simpson, J. H., & Goodman, C. S. (2001). Switching repulsion to attraction: Changing responses to slit during transition in mesoderm migration. *Science (New York, N.Y.), 292*(5517), 737-740. doi:10.1126/science.1058766

Lee, J. K., Coyne, R. S., Dubreuil, R. R., Goldstein, L. S., & Branton, D. (1993). Cell shape and interaction defects in alpha-spectrin mutants of drosophila melanogaster. *The Journal of Cell Biology, 123*(6 Pt 2), 1797-1809.

Legate, K. R., Wickstrom, S. A., & Fassler, R. (2009). Genetic and cell biological analysis of integrin outside-in signaling. *Genes & Development, 23*(4), 397-418. doi:10.1101/gad.1758709

Leptin, M., Bogaert, T., Lehmann, R., & Wilcox, M. (1989). The function of PS integrins during drosophila embryogenesis. *Cell, 56*(3), 401-408.

Lubarsky, B., & Krasnow, M. A. (2003a). Tube morphogenesis: Making and shaping biological tubes. *Cell, 112*(1), 19-28.

Lubarsky, B., & Krasnow, M. A. (2003b). Tube morphogenesis: Making and shaping biological tubes. *Cell, 112*(1), 19-28. doi:DOI: 10.1016/S0092-8674(02)01283-7

MacMullin, A., & Jacobs, J. R. (2006). Slit coordinates cardiac morphogenesis in drosophila. *Developmental Biology, 293*(1), 154-164. doi:10.1016/j.ydbio.2006.01.027

Margadant, C., & Sonnenberg, A. (2010). Integrin-TGF-beta crosstalk in fibrosis, cancer and wound healing. *EMBO Reports, 11*(2), 97-105. doi:10.1038/embor.2009.276

Martin, D., Zusman, S., Li, X., Williams, E. L., Khare, N., DaRocha, S., Chiquet-Ehrismann, R., & Baumgartner, S. (1999). Wing blister, a new drosophila laminin alpha chain required for cell adhesion and migration during embryonic and imaginal development. *The Journal of Cell Biology, 145*(1), 191-201.

Martin-Bermudo, M. D., Dunin-Borkowski, O. M., & Brown, N. H. (1997). Specificity of PS integrin function during embryogenesis resides in the alpha subunit extracellular domain. *The EMBO Journal, 16*(14), 4184-4193.

Martin-Bermudo, M. D., Alvarez-Garcia, I., & Brown, N. H. (1999). Migration of the drosophila primordial midgut cells requires coordination of diverse PS integrin functions. *Development (Cambridge, England), 126*(22), 5161-5169.

Martin-Bermudo, M. D., Dunin-Borkowski, O. M., & Brown, N. H. (1998a). Modulation of integrin activity is vital for morphogenesis. *The Journal of Cell Biology, 141*(4), 1073-1081.

Martin-Bermudo, M. D., Dunin-Borkowski, O. M., & Brown, N. H. (1998b). Modulation of integrin activity is vital for morphogenesis. *The Journal of Cell Biology, 141*(4), 1073-1081. doi:10.1083/jcb.141.4.1073

Medioni, C., Astier, M., Zmojdzian, M., Jagla, K., & Semeriva, M. (2008). Genetic control of cell morphogenesis during drosophila melanogaster cardiac tube formation. *The Journal of Cell Biology, 182*(2), 249-261. doi:10.1083/jcb.200801100

Medioni, C., Senatore, S., Salmand, P. A., Lalevee, N., Perrin, L., & Semeriva, M. (2009). The fabulous destiny of the drosophila heart. *Current Opinion in Genetics & Development, 19*(5), 518-525. doi:10.1016/j.gde.2009.07.004

Qian, L., Liu, J., & Bodmer, R. (2005). Slit and robo control cardiac cell polarity and morphogenesis. *Current Biology : CB, 15*(24), 2271-2278. doi:10.1016/j.cub.2005.10.037

Rajagopalan, S., Vivancos, V., Nicolas, E., & Dickson, B. J. (2000). Selecting a longitudinal pathway: Robo receptors specify the lateral position of axons in the drosophila CNS. *Cell, 103*(7), 1033-1045.

Rothberg, J. M., Jacobs, J. R., Goodman, C. S., & Artavanis-Tsakonas, S. (1990). Slit: An extracellular protein necessary for development of midline glia and commissural axon pathways contains both EGF and LRR domains. *Genes & Development, 4*(12a), 2169-2187. doi:10.1101/gad.4.12a.2169

Rothberg, J. M., Hartley, D. A., Walther, Z., & Artavanis-Tsakonas, S. (1988). Slit: An EGF-homologous locus of D. melanogaster involved in the development of the embryonic central nervous system. *Cell, 55*(6), 1047-1059.

Rugendorff, A., Younossi-Hartenstein, A., & Hartenstein, V. (1994). Embryonic origin and differentiation of the *drosophila* heart. *Developmental Biology,* (203), 266-280.

Santiago-Martinez, E., Soplop, N. H., Patel, R., & Kramer, S. G. (2008). Repulsion by slit and roundabout prevents Shotgun/E-cadherin-mediated cell adhesion during drosophila heart tube lumen formation. *The Journal of Cell Biology, 182*(2), 241-248.

Santiago-Martinez, E., Soplop, N. H., & Kramer, S. G. (2006). Lateral positioning at the dorsal midline: Slit and roundabout receptors guide drosophila heart cell migration. *Proceedings of the National Academy of Sciences of the United States of America, 103*(33), 12441-12446. doi:10.1073/pnas.0605284103

Simpson, J. H., Bland, K. S., Fetter, R. D., & Goodman, C. S. (2000). Short-range and long-range guidance by slit and its robo receptors: A combinatorial code of robo receptors controls lateral position. *Cell, 103*(7), 1019-1032.

Stark, K. A., Yee, G. H., Roote, C. E., Williams, E. L., Zusman, S., & Hynes, R. O. (1997). A novel alpha integrin subunit associates with betaPS and functions in tissue morphogenesis and movement during *drosophila* development. *Development, 124*, 4583-4594.

Steigemann, P., Molitor, A., Fellert, S., Jackle, H., & Vorbruggen, G. (2004). Heparan sulfate proteoglycan syndecan promotes axonal and myotube guidance by slit/robo signaling. *Current Biology : CB, 14*(3), 225-230. doi:10.1016/j.cub.2004.01.006

Stevens, A., & Jacobs, J. R. (2002). Integrins regulate responsiveness to slit repellent signals. *The Journal of Neuroscience : The Official Journal of the Society for Neuroscience, 22*(11), 4448-4455. doi:20026413

Stupack, D. G. (2007). The biology of integrins. *Oncology (Williston Park, N.Y.), 21*(9 Suppl 3), 6-12.

Tao, Y., & Schulz, R. A. (2007). Heart development in drosophila. *Seminars in Cell & Developmental Biology, 18*(1), 3-15.

Tearle, R. G., & Nusslein-Volhard, C. (1987). *Tubingen mutants and stock list*

Tweedie, S., Ashburner, M., Falls, K., Leyland, P., McQuilton, P., Marygold, S., Millburn, G., Osumi-Sutherland, D., Schroeder, A., Seal, R., Zhang, H., & The FlyBase Consortium. (2009). FlyBase: Enhancing drosophila gene ontology annotations. *Nucleic Acids Research, 37*(D555-D559) doi:10.1093/nar/gkn788

Wilcox, M., DiAntonio, A., & Leptin, M. (1989). The function of PS integrins in drosophila wing morphogenesis. *Development (Cambridge, England), 107*(4), 891-897.

Wong, K., Park, H. T., Wu, J. Y., & Rao, Y. (2002). Slit proteins: Molecular guidance cues for cells ranging from neurons to leukocytes. *Current Opinion in Genetics & Development, 12*(5), 583-591.

Woods, D. F., Hough, C., Peel, D., Callaini, G., & Bryant, P. J. (1996). Dlg protein is required for junction structure, cell polarity, and proliferation control in drosophila epithelia. *The Journal of Cell Biology, 134*(6), 1469-1482.

Wu, C. (1997). Roles of integrins in fibronectin matrix assembly. *Histology and Histopathology, 12*(1), 233-240.

Xian, X., Gopal, S., & Couchman, J. R. (2010). Syndecans as receptors and organizers of the extracellular matrix. *Cell and Tissue Research, 339*(1), 31-46. doi:10.1007/s00441-009-0829-3

Yee, G. H., & Hynes, R. O. (1993). A novel, tissue-specific integrin subunit, beta nu, expressed in the midgut of drosophila melanogaster. *Development (Cambridge, England), 118*(3), 845-858.

Yuan, S. S., Cox, L. A., Dasika, G. K., & Lee, E. Y. (1999). Cloning and functional studies of a novel gene aberrantly expressed in RB-deficient embryos. *Developmental Biology, 207*(1), 62-75. doi:10.1006/dbio.1998.9141

Zaffran, S., Reim, I., Qian, L., Lo, P. C., Bodmer, R., & Frasch, M. (2006). Cardioblast-intrinsic tinman activity controls proper diversification and differentiation of myocardial cells in drosophila. *Development (Cambridge, England), 133*(20), 4073-4083. doi:10.1242/dev.02586

Zaidel-Bar, R., Itzkovitz, S., Ma'ayan, A., Iyengar, R., & Geiger, B. (2007). Functional atlas of the integrin adhesome. *Nature Cell Biology, 9*(8), 858-867. doi:10.1038/ncb0807-858

APPENDIX 1

Preliminary Figures

Figures by Allison MacMullin

Figure A1.1: The αPS3 Integrin *scab* Interacts Genetically with *slit* in a Dosage Dependent Manner.

Stage 17 embryos heterozygous for a null allele of *scab* have normal heart development (B) when compared to wild type embryonic heart development (A). Embryos homozygous mutant for *scab* fail to have proper heart development (C). Delays (asterisk), twists (arrow) and ectopic cardial cells (arrowhead) are common defects observed in embryos lacking *scab*. A severe phenotype is also observed in embryos doubly heterozygous for both *slit* and *scab* (D). Twists (arrow), delays (asterisk) and misplaced cardial cells (i.e. clumping and ectopic cells, arrowheads) are commonly seen in double heterozygote embryos. This phenotype is 100% penetrant, however it can vary in severity. In all panels, cardial cells are labelled using β-galactosidase to detect the B2-3-20 cardial cell enhancer. Anterior is to the top.

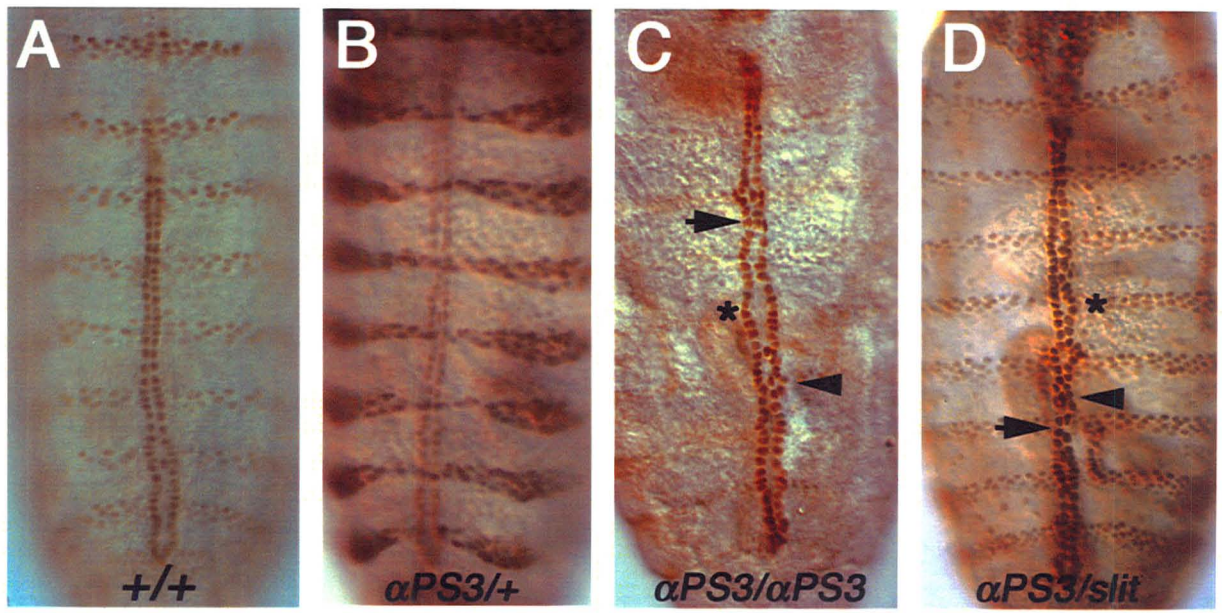
A
+/+
B
αPS3/+
C
αPS3/αPS3
D
αPS3/slit

Figure A1.2: *slit* Interacts in a Dosage Dependent Manner with Genes Required for Adhesion.

Stage 17 embryos heterozygous for *slit* have normal heart development (A), while *sli/sli* embryos have twists (asterisk) and blisters (arrowhead) in the mature dorsal vessel (B). Embryos doubly heterozygous for *slit* and *scab* (C) or *βPS1* (*mys*) (D) have delayed migration (black arrow) and clumping of heart cells (white arrow). Integrin ligands Laminin A (*lanA*) (E), Laminin-α 1,2 (*wb*) (F) and Collagen IV (*vkg*) (G) interact genetically with *slit*, but ECM protein and ligand Tiggrin (*tig*), which does not bind the αPS3βPS1 integrin receptor, does not (H). Defects such as gaps (diamond), delays (white arrow) and twists (asterisk) are observed in embryos heterozygous for *slit* and *lanA, wb* or *vkg.* In all panels, cardial cells are labled using β-galactosidase to detect the B2-3-20 ehancer trap. Anterior is to the top.

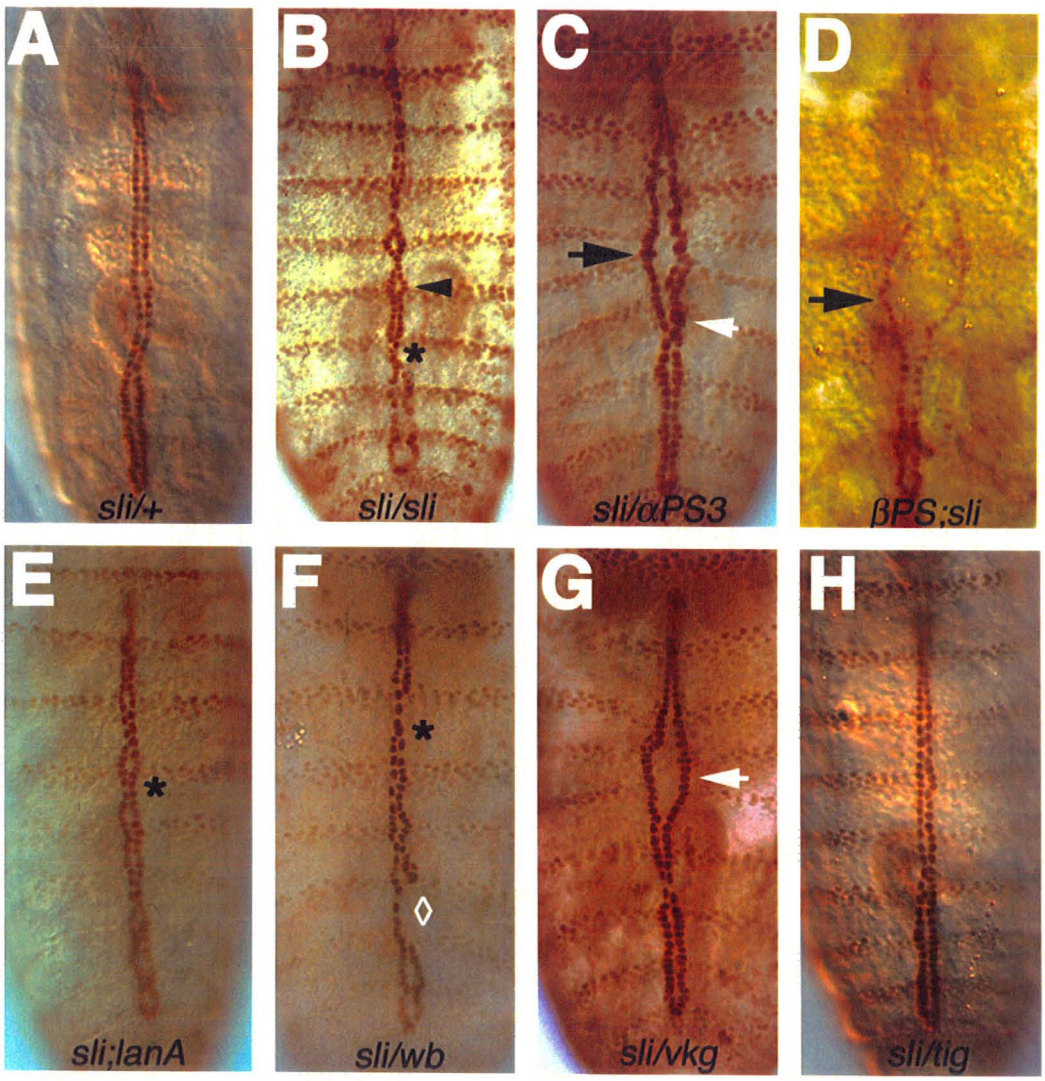
A
sli/+
B
sli/sli
C
sli/αPS3
D
βPS;sli
E
sli;lanA
F
sli/wb
G
sli/vkg
H
sli/tig

Figure A1.3: *slit* Interacts Genetically with Downstream Effectors of Integrin Function.

Talin (*rhea*) and Integrin Linked Kinase (*ILK*) were observed to have heart defects in embryos doubly heterozygous for one of these genes and *slit.* Embryos heterozygous for *slit* have no visible phenotype (A). Embryos doubly heterozygous for both *sli* and *ILK* have a delay in the migration of the cardial cells (arrow) as well as a twist in the dorsal vessel (arrowhead) (B). Embryos doubly heterozygous for both *sli* and *rhea* (*talin*) have a more minor phenotype, with visible gaps in the continuity of the cardial cells (asterisk) (C). Cardial cells are labeled with β-galactosidase to detect the B2-3-20 cardial cell enhancer trap. Anterior is to the top.

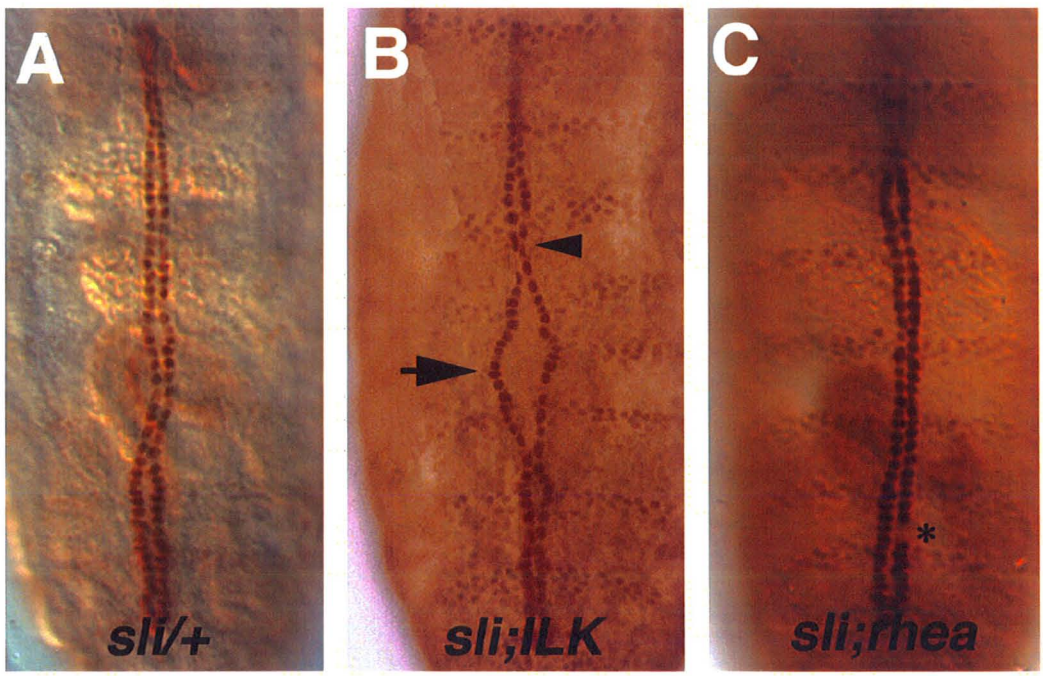
A
sli/+
B
sli;ILK
C
sli;rhea

Figure A1.4 Integrins function to coordinate cardial cell morphogenesis in an adhesive nature.

Embryos heterozygous for *scab* have normal cardial cell morphogenesis (A), while those lacking αPS3 have severe defects in heart development, including gaps (arrow), twists (arrowhead) and misplaced/ectopic cells (asterisk) (B). Embryos doubly heterozygous for *αPS3* and *lanA*, the αPS3/βPS1 receptor ligand, also have a severe heart assembly phenotype, with several twists (arrow) and misplaced cells prominent (arrowhead) (C). Embryos doubly heterozygous for genes required for the adhesive properties of integrins (Laminin α1,2 (*wb*), Collagen IV (*vkg*) and integrin ligand Tiggrin (*tig)*) and *αPS3* have severe perturbations in cardial cell structure (D, E, F. respectively). Large gaps in cardial cell continuity are seen (diamond), as well as misplaced cells (black arrow), ectopic cardial cells (white arrow), twisting (arrowhead) and delays (asterisk) in the migration of the cells towards the dorsal midline. Cardial cells are visualized using α-β-galactosidase to detect the cardial cell enhancer trap, B2-3-20. In all panels, anterior is to the top.

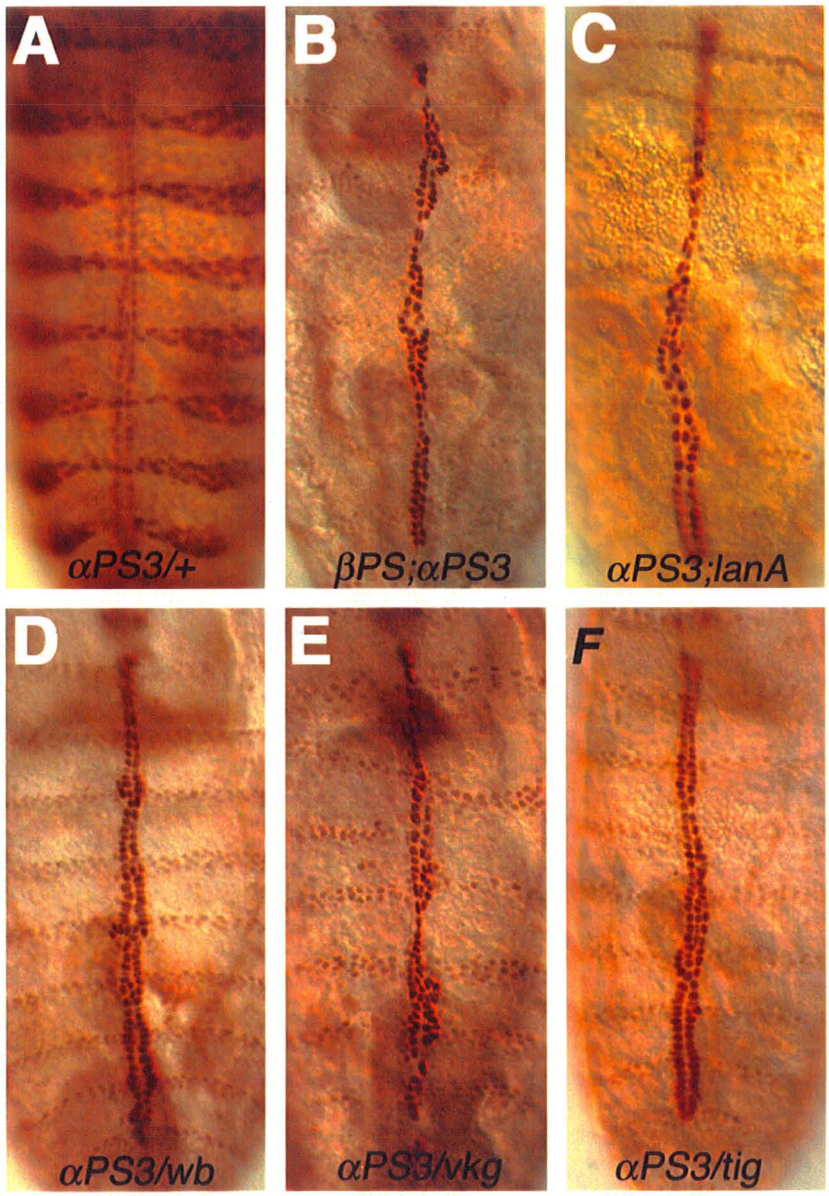
A
αPS3/+
B
βPS;αPS3
C
αPS3;lanA
D
αPS3/wb
E
αPS3/vkg
F
αPS3/tig

Figure A1.5: The αPS3 Integrin *scab* Interacts Genetically with Genes Required for Robo Signaling.

To further assess the role integrin signaling and adhesion have in cardiac development and how they may modify Slit signaling, embryos doubly heterozygous for *scb* and genes required for Robo signaling were assayed for a potential genetic interaction. Embryos heterozygous for *scb* (A) appear wild type. Interestingly, embryos doubly heterozygous for *scb* and *leak* (*Robo2*) have noticeable perturbations in the dorsal vessel, including a gap in the line of cardial cells (diamond) and clumped and/or ectopic cardial cells (arrowhead) (B). This is a stark contrast to the minor genetic interaction observed between *slit* and *leak*. Genes required for second messenger signaling downstream of Robo also showed noticeable genetic interactions with *scb* in the developing dorsal vessel (C, D, E). Embryos doubly heterozygous for *scb* and *dock*, *Drosophila Nck*, have a very visible phenotype, with the presence of a large gap (arrow) and delays in the migration of the cardial cells towards the dorsal midline (asterisk) (C). *scb* and *dab* (*disabled*), an adaptor protein involved in Robo signaling, have a fairly severe phenotype, with some twists in the mature heart visible (black arrow), large delays in migration (black arrowhead), ectopic cardial cells (white arrow) and elongated cardial cells (white arrowhead) (D). Lastly, embryos doubly heterozygous for *slit* and *abl*, a tyrosine kinase involved in Robo signaling, have a minor phenotype with some ectopic and elongated cells visible (arrow and arrowhead, respectively) (E). Cardial cells were visualized with α-β-galactosidase to detect the B2-3-20 enhancer trap. Anterior is to the top of all panels.

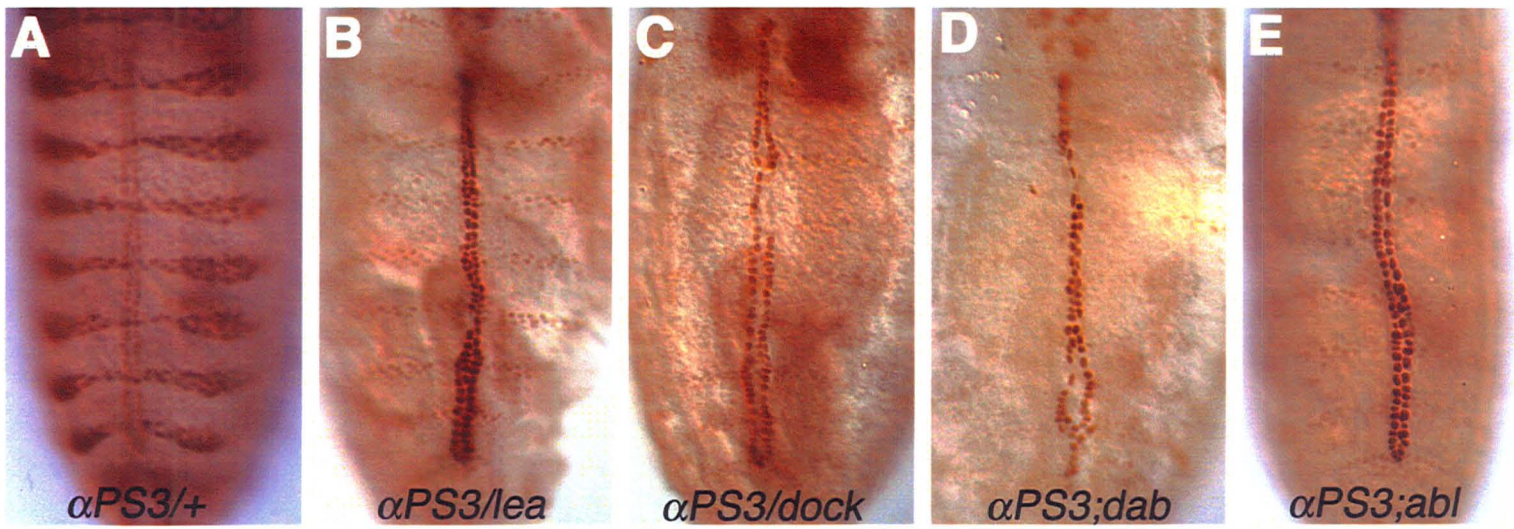
A
αPS3/+
B
αPS3/lea
C
αPS3/dock
D
αPS3;dab
E
αPS3;abl

Figure A1.6: The *sli/αPS3* Dorsal Vessel Phenotype is not due to a Defect in Dorsal Closure.

PhosphoTyrosine labeling (red) and cardial cell labeling (green) were used to assay the affects of dorsal closure on dorsal vessel formation. In wild type (A) and *slit* (C) stage 14 embryos, cardial cells are 1 to 2 cell diameters away from the aminoserosa (arrow, as). Dorsal closure is complete in wild type (A) and *slit* embryos (D) by stage 17. In contrast, the cardial cells of αPS3 (*scab*) mutants are adjacent to the aminoserosa at stage 15 (E, arrow) and 17 (F, arrow), and dorsal closure is incomplete by stage 17. Embryos doubly heterozygous for *slit* and αPS3 have an intermediate phenotype at stage 15, with the cardial cells lying just beneath the leading edge cells (G, arrowhead). Dorsal closure is delayed, but complete at hatching (H).

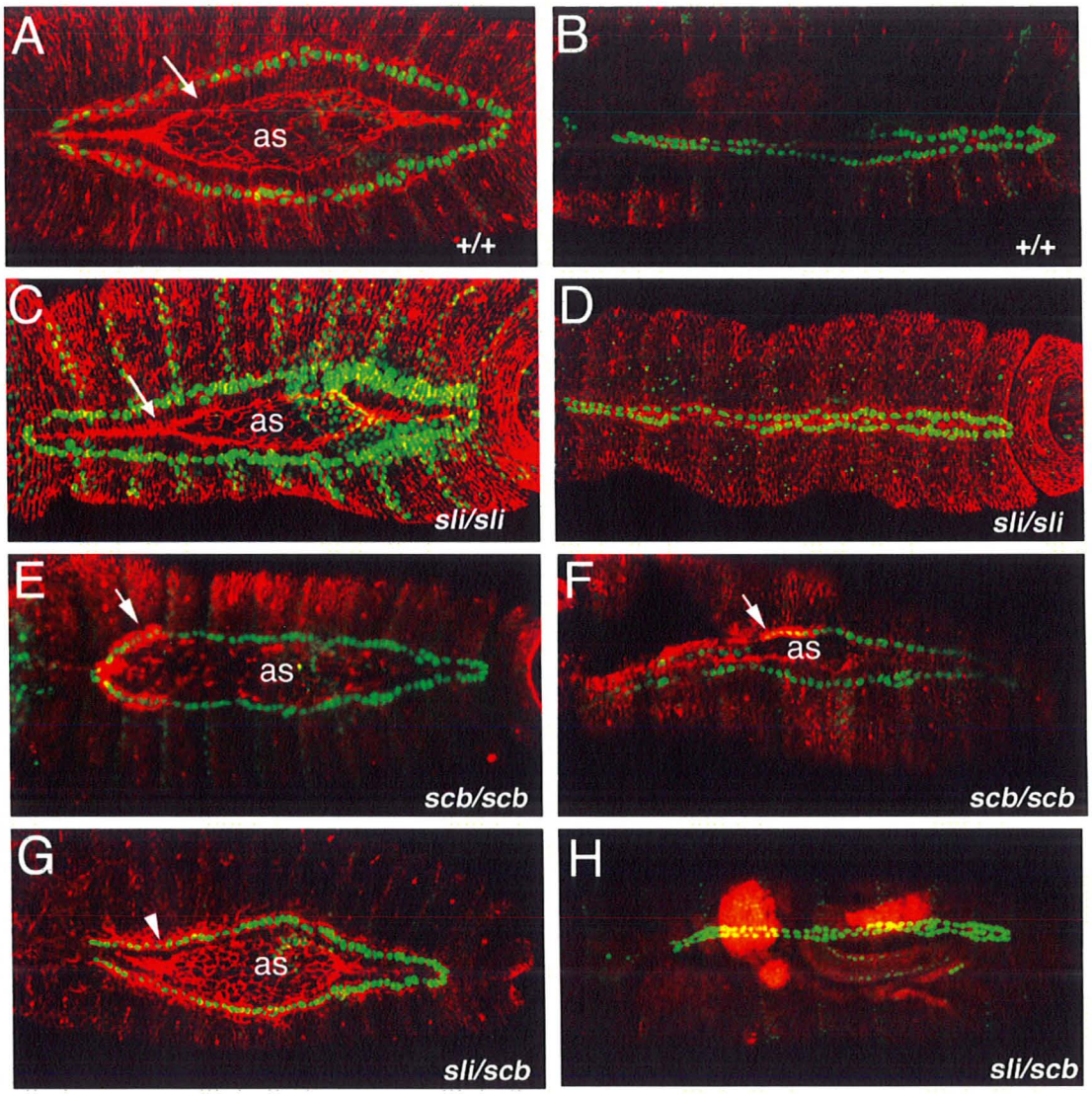
A
as
+/+
B
+/+
C
as
sli/sli
D
sli/sli
E
as
scb/scb
F
as
scb/scb
G
as
sli/scb
H
sli/scb

APPENDIX 2

Supplementary Data

by Luz de Lourdes Vazquez Paz

Figure A2.1: Slit and Robo localization in wild type and *scb01288*

Analysis of Slit and Robo localization in the hypomorphic allele *scab01288*. In wild type embryos Robo [A] and Slit [B] accumulate apically in the lumen where little lateral signal is observed. In contrast, *scb01288* mutant embryos reveal lateral accumulation of Robo and Slit between the cardioblasts in the absence of the aPS3 integrin (arrows) [C-D]. A reduction in signal of Robo [C] and Slit [D] as compared to their wild type counterparts is observed. This data is in agreement with the phenotypes observed with the null allele of *scab* (*scb2*). Dorsal view of stage 16-17 wild type [A-B] and *scb01288* mutant [C-D] embryos immunolabelled using anti-β-galactosidase to detect the B2-3-20 cardial cell enhancer trap (green) and MAb to detect Slit and Robo (red) imaged using confocal microscopy. Posterior of the heart is seen (anterior to the left). Calibration: 5μm

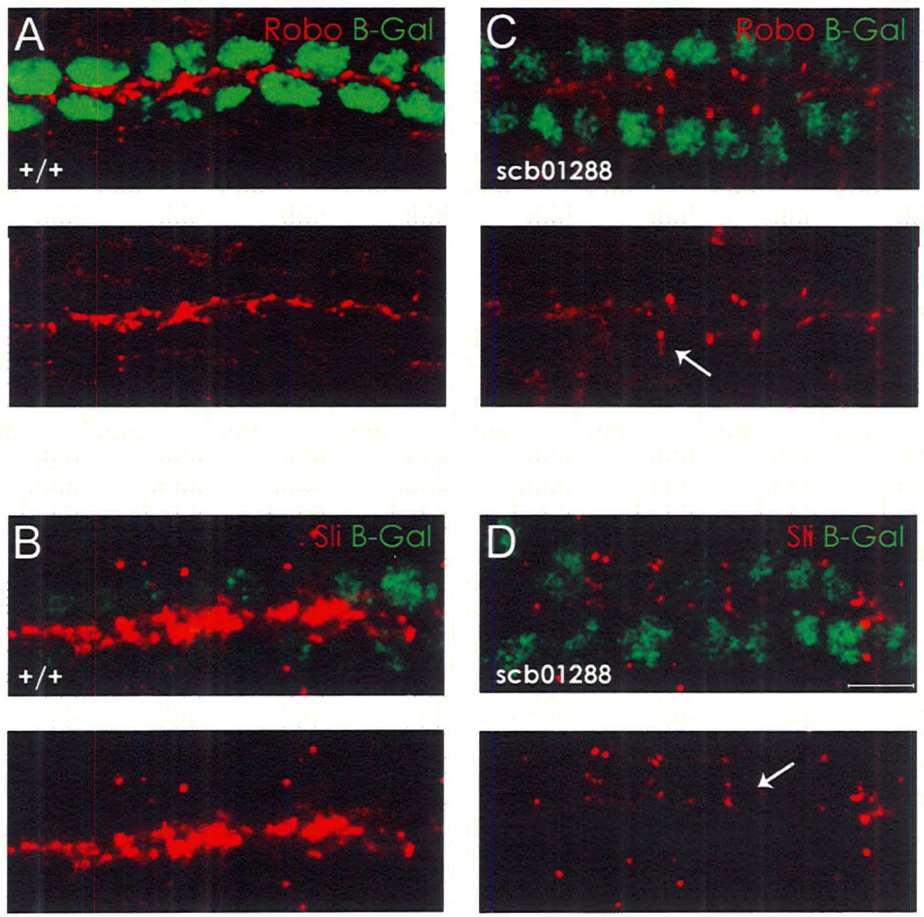
A
Robo B-Gal
+/+
C
Robo B-Gal
scb01288
B
Sli B-Gal
+/+
D
Sli B-Gal
scb01288

Figure A2.2: Characterization of the αPS3 polyclonal antibody

A rabbit polyclonal antibody against the N-terminus of αPS3 was generated using a His-tagged protein. Following serum preparation the antibody was tested by immunoblot and immunohistochemistry. The molecular weight of αPS3 is estimated to be ~125kDa.

[A] αPS3 was induced after HS in *w-;HSP70-GAL4;UAS-scb* adult flies (*w-;CyO;UAS-scb* used as an internal negative control). Immunoblotting was performed on extracts from head tissue without (0h) or after 3h HS. Western blots containing ~60μg of protein per lane were incubated with the serum generated against αPS3. This antiserum recognizes the over-expressed protein (~125kDa) but fails to recognize the endogenous protein. [B] αPS3 was expressed using the ubiquitous driver *da-GAL4*. Immunoblotting was performed on head tissue extracts of *da-GAL4/UAS-scab* or *UAS-scab* flies. Western blots containing varying amounts of the endogenous protein were incubated with the serum (1:50,000). The antiserum recognizes the over-expressed protein (~125kDa) but fails to recognize the endogenous protein. In both immunoblots an unidentified band (~150kDa) is recognized suggesting cross-reaction or unspecific binding. [C] Over-expression with the muscle specific driver *dMef-GAL4* of the *scab* transgene is recognized by the antibody. However, in wild type embryos the αPS3 antiserum fails to provide a specific signal of the integrin as it cannot be observed in the heart nor the amnioserosa. Together this data suggest that the antiserum generated does not recognize endogenous αPS3.

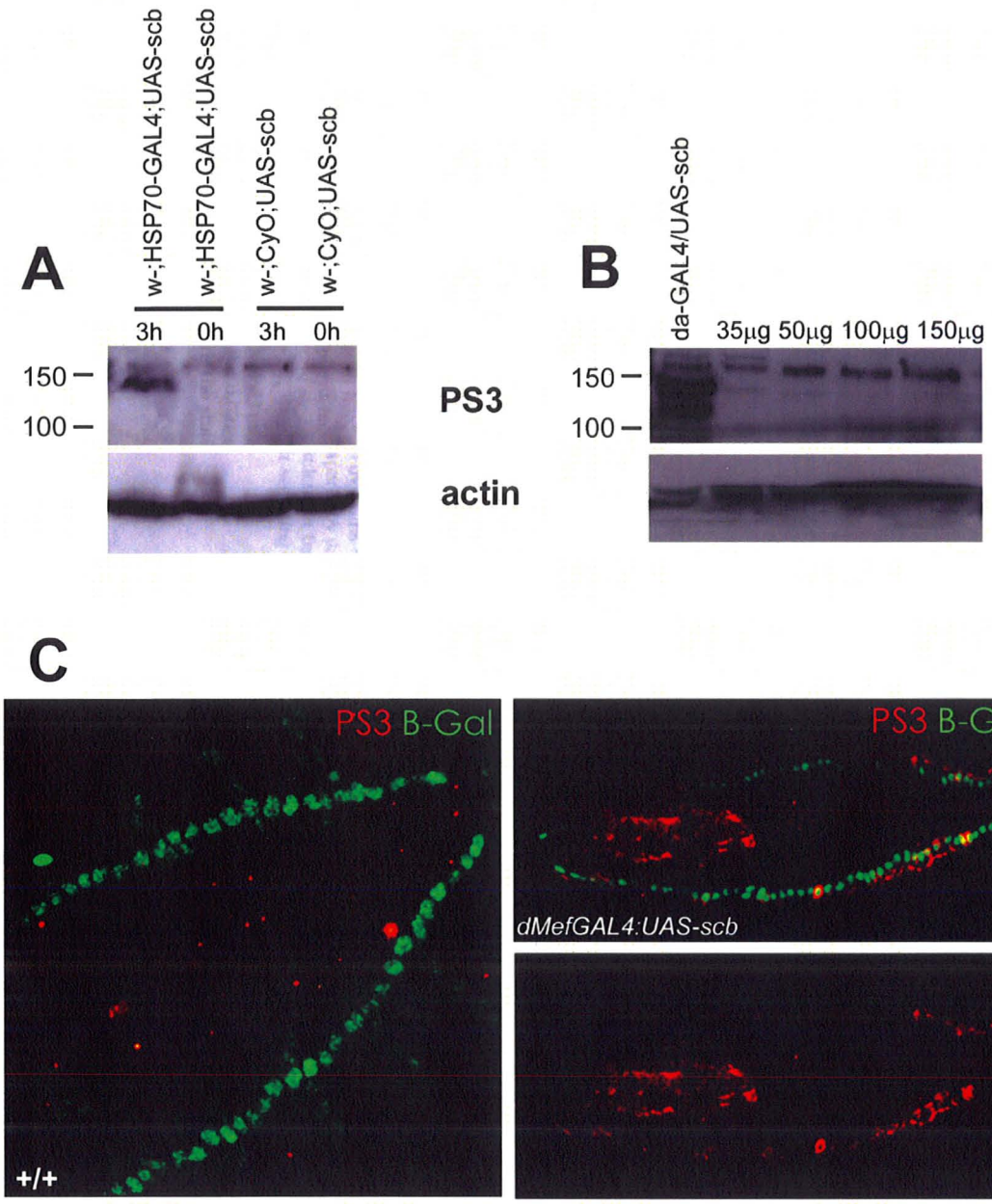
A
w-;HSP70-GAL4;UAS-scb
w-;HSP70-GAL4;UAS-scb
w-;CyO;UAS-scb
w-;CyO;UAS-scb
3h
0h
3h
0h
150
100
PS3
actin
B
da-GAL4/UAS-scb
35µg 50µg 100µg 150µg
150
100
C
PS3 B-Gal
+/+
PS3 B-Gal
dMefGAL4:UAS-scb

Figure A2.3: RNAi mediated knockdown of αPS3 and βPS1

Stage 16-17 embryos over-expressing a dsRNA construct using the muscle specific driver dMef-GAL4. All embryos were kept at 29°C to ensure a maximal over-expression of the dsRNA constructs. [A] *scab-RNAi* over-expression (*scabRNAi;dMef-GAL4*) alters heart assembly ranging from mild phenotypes (left) to more severe ones (right) with a penetrance of 60%. [B] Similar results can be observed when *mys-RNAi* is over-expressed (*UAS-mysRNAi;dMef-GAL4*). Mild phenotypes where dorsal vessel assembly is not significantly altered as compared to wild type are most common. Severe phenotypes are not as common and often display irregular and delayed migration.

(C) Western blots containing ~150µg of *UAS-scab/da-GAL4*, *UAS-scabRNAi* or *UAS-scabRNAi/da-GAL4* embryonic protein lysate were incubated with the serum generated against αPS3 (1:50,000). This antiserum recognizes the over-expressed full-length protein (~125kDa) but not the endogenous protein. Without a baseline signal, knockdown of αPS3 was inconclusive. **(D)** Immunolabelling of βPS1 in an embryo over-expressing *UAS-mysRNAi* using the muscle specific driver *dMef-GAL4*. Strong levels of βPS1 can be observed throughout the musculature of the embryo suggesting a lack of protein knockdown. Embryos were immunolabelled using a MAb for βPS1 (red) and antiserum raised against dMEF2 (green).

A


dMef-GAL4:UAS-scbRNAi

B

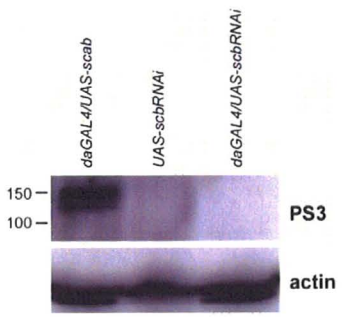
daGAL4/UAS-scab
UAS-scbRNAi
daGAL4/UAS-scbRNAi
150
100
PS3
actin

C


dMef-GAL4:UAS-mysRNAi

D

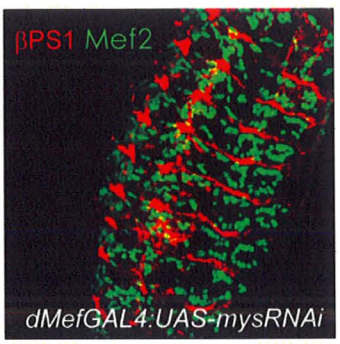
βPS1 Mef2
dMefGAL4:UAS-mysRNAi

Figure A2.4 Localization of the cell junctional marker Par6

A GFP-tagged Par6 fusion protein was over-expressed in wild type [A] and *scb2* [B] backgrounds using the muscle specific driver *dMef-GAL4*. In polarized epithelia Par 6 localizes to the apical-lateral surface of cells. In cardioblasts, the over-expressed protein is seen over the entire surface of the cell yielding little information on the polarization of this marker. Cardial cells are labelled using anti-β-Galactosidase to detect the B2-3-20 cardial cell enhancer trap and anti-GFP to detect the Par6GFP fusion protein.

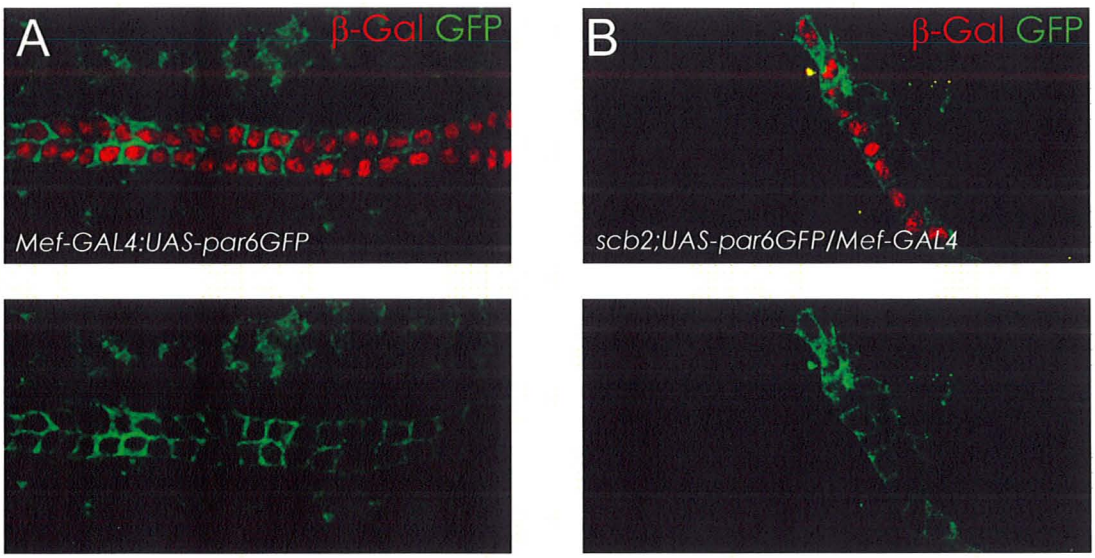
A
β-Gal GFP
Mef-GAL4:UAS-par6GFP
B
β-Gal GFP
scb2;UAS-par6GFP/Mef-GAL4

Figure A2.5 Sequence Alignment pUAST-scab and CDS

Sequence alignment showing the published CDS in FlyBase and the sequence obtained from pUAST-scab using the same primers used to clone the antigenic fusion protein. Only a small portion of the alignment is shown here where the 18 base pair gap can be seen. Alignment of the two sequences was done using the ClustalW alignment tool.

```
FlyBase         GTTTCGAGGGGAGCAGTTTGGCGAATACTTTGGGTACTCCGTTCTGGCGGAAGATCTAAA 1079
pUAST-scab      GTTTCGAGGGGAGCAGTTTGGCGAATACTTTGGGTACTCCGTTCTGGCGGAAGATCTAAA 1015
TA-scab         GTTTCGAGGGGAGCAGTTTGGCGAATACTTTGGGTACTCCGTTCTGGCGGAAGATCTAAA 984
                ************************************************************

FlyBase         TGGAGACGGGAAAACGGATGTTATCGTATCAGCGCCACAGCACGCTCTGGAGGATTCCCA 1139
pUAST-scab      TGGAGACGGGAAAACGGATGTTATCGTATCAGCGCCACAGCACGCTCTGGAGGATTCCCA 1075
TA-scab         TGGAGACGGGAAAACGGATGTTATCGTATCAGCGCCACAGCACGCTCTGGAGGATTCCCA 1044
                ************************************************************

FlyBase         CGACAACGGTGCCATCTACGTGTTCATCAACAAAGGCTTTTTCAACTTTGAACGGCAGAT 1199
pUAST-scab      CGACAACGGTGCCATCTACGTGTTCATCAACAAAGGCTTT------------------AT 1117
TA-scab         CGACAACGGTGCCATCTACGTGTTCATCAACAAAGGCTTT------------------AT 1086
                ****************************************                  **

FlyBase         TTTGCGTTCGCCAGTGGAGACTATGGCGCGTTTCGGCACTGCTCTATCGCGTCTTGGAGA 1259
pUAST-scab      TTTGCGTTCGCCAGTGGAGACTATGGCGCGTTTCGGCACTGCTCTATCGCGTCTTGGAGA 1177
TA-scab         TTTGCGTTCGCCAGTGGAGACTATGGCGCGTTTCGGCACTGCTCTATCGCGTCTTGGAGA 1146
                ************************************************************

FlyBase         TATTAATCACGATGGGTATAATGATGTGGCAGTTGGAGCTCCTTTTGCTGGAAATGGAAC 1319
pUAST-scab      TATTAATCACGATGGGTATAATGATGTGGCAGTTGGAGCTCCTTTTGCTGGAAATGGAAC 1237
TA-scab         TATTAATCACGATGGGTATAATGATGTGGCAGTTGGAGCTCCTTTTGCTGGAAATGGAAC 1206
                ************************************************************

FlyBase         GGTGTTTATCTACCTAGGCAGCGAAAATGGATTACGAGATCAGCCGAGTCAGCGCCTGGA 1379
pUAST-scab      GGTGTTTATCTACCTAGGCAGCGAAAATGGATTACGAGATCAGCCGAGTCAGCGCCTGGA 1297
TA-scab         GGTGTTTATCTACCTAGGCAGCGAAAATGGATTACGAGATCAGCCGAGTCAGCGCCTGGA 1266
                ************************************************************

FlyBase         TGCTCCTTCCCAGCAACCCTCCAAGTACGGATCGCACATGTTCGGCCACGGGCTGTCCCG 1439
pUAST-scab      TGCTCCTTCCCAGCAACCCTCCAAGTACGGATCGCACATGTTCGGCCACGGGCTGTCCCG 1357
TA-scab         TGCTCCTTCCCAGCAACCCTCCAAGTACGGATCGCACATGTTCGGCCACGGGCTGTCCCG 1326
                ************************************************************

FlyBase         TGGATCCGACATAGATGGCAACGGATTCAACGACTTTGCCATTGGAGCTCCAAATGCGGA 1499
pUAST-scab      TGGATCCGACATAGATGGCAACGGATTCAACGACTTTGCCATTGGAGCTCCAAATGCGGA 1417
TA-scab         TGGATCCGACATAGATGGCAACGGATTCAACGACTTTGCCATTGGAGCTCCAAATGCGGA 1386
                ************************************************************
```

Table A2.3 Adult Viability Analysis of RNAi Over-Expression at 29°C

UAS-scbRNAi X dMef-GAL4		*UAS-scbRNAi X da-GAL4*	
Male	**Female**	**Male**	**Female**
52	60	0	0
112		Pupal Lethal	

UAS-mysRNAi X dMef-GAL4		*UAS-mysRNAi X da-GAL4*	
Male	**Female**	**Male**	**Female**
47	61	0	0
108		Larval Lethal	

Table A2.4 RNAi Embryonic Lethality

Genotype	*UAS-scbRNAi;da-GAL4*	*UAS-mysRNAi;da-GAL4*	*UAS-scbRNAi;dMef2-GAL4*	*UAS-mysRNAi;dMef2-GAL4*
% Lethality	**5.10**	**10.6**	**1.85**	**7.06**
Hatched	93	84	106	79
Unhatched	5	10	2	6
Unfertilized	22	26	12	35
Total	120	120	120	120

Table A2.2: Adult Viability Analysis of Transgene Over-Expression in a *scb2* background

$scb^2/CyOz;UAS\text{-}scb$ X $scb^2/CyOz;dMef\text{-}GAL4, B2\text{-}3\text{-}20/+$			
$scb^2/scb^2;UAS\text{-}scb$ /dMef-GAL4, B2-3-20		$scb^2/scb^2;UAS\text{-}scb$ /+	
Male	**Female**	**Male**	**Female**
0	0	0	0
0		0	
$scb^2/CyOz;UAS\text{-}scb$/dMef-GAL4, B2-3-20		$scb^2/CyOz;UAS\text{-}scb$/+	
Male	**Female**	**Male**	**Female**
62	57	54	70
119		124	
$UAS\text{-}scb\Delta C;scb^2/CyOz/+$ (f) X+;$scb^2/CyOz$; dMef-GAL4, B2-3-20/+			
$UAS\text{-}scb\Delta C/+;scb^2/scb^2;dMef\text{-}GAL4,B2\text{-}3\text{-}20/+$		$UAS\text{-}scb\Delta C/+;\ scb^2/scb^2;$ +	
Male	**Female**	**Male**	**Female**
0	0	0	0
0		0	
$UAS\text{-}scb\Delta C/+;scb^2/CyOz;dMef\text{-}GAL4,B2\text{-}3\text{-}20/+$		$UAS\text{-}scb\Delta C/+;\ scb^2/CyOz/;$ +	
Male	**Female**	**Male**	**Female**
0	0	61	58
0		119	

Table A2.1: Adult Viability Analysis of Transgene Over-Expression

scb²/CyOz;UAS-scb X dMef-GAL4, B2-3-20/TM3							
scb²/+;UAS-scb /dMef-GAL4, B2-3-20		*scb²/+;UAS-scb /TM3*		*+/CyOz;UAS-scb/dMef-GAL4, B2-3-20*		*+/CyOz;UAS-scb/TM3*	
Male	**Female**	**Male**	**Female**	**Male**	**Female**	**Male**	**Female**
29	31	27	20	41	30	27	35
60		47		71		62	

scb²/CyOz;UAS-scb X da-GAL4			
scb²/+;UAS-scb /da-GAL4		*+/CyOz;UAS-scb/da-GAL4*	
Male	**Female**	**Male**	**Female**
34	49	37	36
83		73	

UAS-scbΔC;scb²/CyOz(f) X dMef-GAL4, B2-3-20/TM3							
UAS-scbΔC/+;scb/+²;dMef-GAL4, B2-3-20/+		*UAS-scbΔC/+;scb²/+;TM3/+*		*UAS-scbΔC/+;CyOz/+;dMef-GAL4, B2-3-20/+*		*UAS-scbΔC/+;CyOz/+;TM3/+*	
Male	**Female**	**Male**	**Female**	**Male**	**Female**	**Male**	**Female**
0	0	64	80	0	0	40	63
0		144		0		103	

UAS-scbΔC;scb²/CyOz(f) X da-GAL4			
UAS-scbΔC/+;scb²/+;da-GAL4/+		*UAS-scbΔC/+;CyOz/+;da-GAL4/+*	
Male	**Female**	**Male**	**Female**
0	0	0	0
0		0	